Review: Regional land subsidence accompanying groundwater extraction

Devin L. Galloway · Thomas J. Burbey

Abstract The extraction of groundwater can generate land subsidence by causing the compaction of susceptible aquifer systems, typically unconsolidated alluvial or basin-fill aquifer systems comprising aquifers and aquitards. Various ground-based and remotely sensed methods are used to measure and map subsidence. Many areas of subsidence caused by groundwater pumping have been identified and monitored, and corrective measures to slow or halt subsidence have been devised. Two principal means are used to mitigate subsidence caused by groundwater withdrawal—reduction of groundwater withdrawal, and artificial recharge. Analysis and simulation of aquifer-system compaction follow from the basic relations between head, stress, compressibility, and groundwater flow and are addressed primarily using two approaches—one based on conventional groundwater flow theory and one based on linear poroelasticity theory. Research and development to improve the assessment and analysis of aquifer-system compaction, the accompanying subsidence and potential ground ruptures are needed in the topic areas of the hydromechanical behavior of aquitards, the role of horizontal deformation, the application of differential synthetic aperture radar interferometry, and the regional-scale simulation of coupled groundwater flow and aquifer-system deformation to support resource management and hazard mitigation measures.

Received: 25 March 2011 / Accepted: 24 July 2011
Published online: 26 August 2011

D. L. Galloway (✉)
US Geological Survey,
3020 State Univ. Dr. E, Sacramento, CA 95819, USA
e-mail: dlgallow@usgs.gov

T. J. Burbey
Virginia Tech,
4044 Derring Hall, Blacksburg, VA 24061, USA
e-mail: tjburbey@vt.edu

Keywords Review · Subsidence · Aquifer-system compaction · Numerical modeling · InSAR

Introduction

The term land subsidence includes both gentle downwarping and the sudden sinking of discrete segments of the ground surface. Displacement is principally downward, though associated horizontal deformation often has significant damaging effects. The extraction of groundwater plays a direct role in land subsidence by causing the compaction of susceptible aquifer systems (Fig. 1). Subsidence accompanying the extraction of fluids such as water, crude oil and natural gas from subsurface formations perhaps is the best understood of all causes of land subsidence—anthropogenic and natural. Many areas of subsidence caused by pumping of subsurface fluids have been identified, surface and subsurface changes have been monitored, and corrective measures have been devised. Decades ago, the topic of "land subsidence due to fluid withdrawal" was reviewed by Poland and Davis (1969).

"Land subsidence" in general was included in the United Nations Educational, Scientific and Cultural Organization (UNESCO) program of the International Hydrological Decade, 1965–1974. During the Decade, UNESCO organized the 1st International Symposium on Land Subsidence. In 1975 UNESCO formed the Working Group on Land Subsidence that subsequently produced the *Guidebook to Studies of Land Subsidence Due to Ground-water Withdrawal* (Poland 1984). Eight international symposia on land subsidence have been convened. Proceedings of the symposia comprise numerous scientific papers covering the various types of subsidence identified throughout the world (Tison 1969; IAHS 1977; Johnson et al. 1986; Johnson 1991; Barends et al. 1995; Carbognin et al. 2000; Zhang et al. 2005; Carreón-Freyre et al. 2010) and constitute a rich source of research and case study on subsidence attributed to groundwater extraction. Other useful compilations provide important information on subsidence caused by groundwater extraction (including Holzer 1984a; Singh and Saxena 1991; Prince et al. 1995; Prince and Leake 1997; Borchers 1998; Galloway et al. 1999; Prince and Galloway 2003, and Galloway et al. 2008). Gambolati et al. (2005) present an excellent overview of the occurrences, measurement, mechanisms,

 DOI 10.1007/s10040-011-0775-5

Fig. 1 Photo taken at approximate location of maximum measured subsidence in the San Joaquin Valley near Mendota, California. Land surface subsided approximately 9 m from 1925 to 1977 attributed to aquifer-system compaction caused by groundwater withdrawal. Signs on the pole are positioned at the approximate former elevations of the land surface in 1925 and 1955. Pictured is Dr. J.F. Poland; photograph by R.L. Ireland, USGS, ca. 1977

prediction and remediation of anthropogenic land subsidence caused by the removal of subsurface fluids (groundwater, oil and gas).

The Panel on Land Subsidence of the US National Research Council (1991) recognized three information needs to improve subsidence mitigation: "First, basic earth-science data and information on the magnitude and distribution of subsidence […] to recognize and to assess future problems. […] Second, research on subsidence processes and engineering methods for dealing with subsidence […] for cost-effective damage prevention or control. […] And third, although many types of mitigation methods are in use in the United States, studies of their cost-effectiveness would facilitate choices by decision makers." Mitigation measures have been taken in many subsidence-affected areas. The two principal methods used to mitigate subsidence in these areas may be summarized simply as (1) reduction of groundwater withdrawal through conjunctive use, conservation, and regulation; and (2) artificial recharge of groundwater (Poland 1984). Where these methods have been put into practice, detailed hydrogeologic studies, subsidence monitoring and mapping, and generally analysis and simulation of subsidence preceded their implementation. This paper presents an extensive review of subsidence research and applications pertaining to aquifer-system compaction that accompanies the extraction of groundwater. The review addresses the first and second information needs identified by the Panel on Land Subsidence.

Detection and assessment

Subsidence caused by groundwater withdrawal and compaction of susceptible aquifer systems often is a subtle phenomenon. The problem of detection in regional land subsidence is compounded by the large areal scale of the elevation changes and the requirement for vertically stable reference marks—bench marks—located outside the area affected by subsidence. Two types of ground motion typically occur in susceptible aquifer systems—deformation, and ground failures. Deformation in the form of vertical and horizontal displacement of the land surface is the principal hazard associated with groundwater extraction. Ground failures such as earth fissures and surface faults are associated with areas of differential (vertical) ground displacement (Holzer 1984b) and both horizontal and vertical deformation of the aquifer system which may not be associated with differential (vertical) ground displacement (Helm 1994; Sheng et al. 2003).

Ancillary or anecdotal information that suggests subsidence may be occurring often is useful and pertinent to regional-scale subsidence processes especially where the subsidence is subtle. Some types of ancillary/anecdotal information that have proven useful in identifying susceptible groundwater basins include increased incidence of damaged wells—protruding and (or) collapsed well casings; repeat adjustments to local geodetic controls; riverine or coastal flooding; conveyance and drainage problems; and ground failures (Galloway et al. 2008, pp. 60–67).

Subsidence assessments typically address the spatial changes (magnitude and direction) in the position of land surface, and the process causing the subsidence. Measuring and monitoring subsidence is critical to constrain analyses and forecasts of future subsidence. Computer models of aquifer-system deformation, constrained by the available data, often are used to assess present and potential future hazards.

 DOI 10.1007/s10040-011-0775-5

Measurement, mapping and monitoring

Various methods are used for measuring and mapping spatial gradients and temporal rates of regional and local subsidence and horizontal ground motion (Galloway et al. 1999). The methods generally measure relative changes in the position of the land surface. The observable position typically is a geodetic reference mark that has been established so that any movement can be attributed to deep-seated ground movement rather than surficial effects. Land subsidence has been measured using repeat surveys of bench marks referenced to a known, and presumed stable, reference frame. In many affected areas an accurate assessment has been hindered or delayed by the lack of a sufficiently stable vertical reference frame (control). Table 1 shows some fairly recent measured subsidence rates (local maxima) for select locations throughout the world.

Ground-based geodetic surveys and techniques

Before the advent of the satellite-based global positioning system (GPS) in the 1980s, the most common means of conducting land surveys involved either the theodolite (used to precisely measure vertical and horizontal angles) or, since the 1950s, geodetic distance meters (electronic distance measuring devices, or EDMs). If only vertical position were sought, differential leveling (using automatic levels and graduated rods or digital levels and bar-scale reading rods) has been the method of choice. When surveying to meet the standards set for even the lower orders (second and third) of accuracy in geodetic leveling, 10–15 mm changes in elevation routinely can be measured over distances of kilometers and 1–2 mm of elevation change over a few kilometers can be obtained with the highest quality (first order) of leveling. When the length of the survey is small (about 10 km or less) differential leveling still is commonly used because it can be both accurate and economical. However, proven high quality (first-order) leveling is tedious, time-consuming, and costly. Large regional networks may warrant use of GPS or airborne and space-based geodetic surveys. If more precise and accurate measurements of change are needed on a local scale, extensometers may be used. If more spatial detail is required over short distances, tripod-mounted LiDAR (light detection and ranging), and ground-based differential interferometry using real aperture radar (Werner et al. 2008) and synthetic aperture radar techniques (Leva et al. 2003) may be used. Optical techniques using combined fringe projection and speckle photography on bench-scale laboratory models of deforming earth materials show promise in elucidating three-dimensional (3D) deformation processes in granular media (Barrientos et al. 2008). Details on the ground-based interferometric and the bench-scale optical techniques are not covered further in this review.

Precise differential leveling

Historically, the elevation of bench marks at land surface commonly has been determined using precise differential leveling. Procedures or specifications are described in detail in the National Oceanic and Atmospheric Administration (NOAA)'s Manual NOS NGS 3, *Geodetic Leveling* (Schomaker and Berry 1981). Once a monitoring network of bench marks has been established and surveyed, repeat surveys at later dates show the location and magnitude of vertical movement if any has occurred.

Typically, the monitoring network is designed to cover the known or suspected subsiding area, and includes stable reference marks that are part of a broader regional geodetic control network. Spacing of bench marks normally is as much as about 1,600 m, but typically is much smaller in areas of special interest. Details on installation and protection of bench marks are available in NOAA Manual NOS NGS 1, *Geodetic Bench Marks* (Floyd 1978).

Traditionally, in bench mark surveys of subsiding areas, leveling has been done to first or second order standards,

Table 1 Recent measured subsidence rates for select locations. Rates represent the local maximum measured rate for the specified period

Location	Rate (mm/yr)	Period	Measurement method	Source
Bangkok, Thailand	30	2006	Leveling	Phien-wej et al. (2006)
Bologna, Italy	40	2002–2006	Differential interferometry	Bonsignore et al. (2010)
Changzhou, Peoples Republic of China	10	2002	Leveling	Wang et al. (2009)
Coachella Valley, California, US	70	2003–2009	Differential interferometry	Sneed (2010)
Datong, Peoples Republic of China	20	2004–2008	Differential interferometry	Zhao et al. (2011)
Houston-Galveston, Texas, US	40	1996–1998	Differential interferometry	Buckley et al. (2003)
Jakarta, Indonesia	250	1997–2008	Global positioning system	Abidin et al. (2009)
Kolkata, India	6	1992–1998	Differential interferometry	Chatterjee et al. (2006)
Mashhad Valley, Iran	280	2003–2005	Differential interferometry	Motagh et al. (2007)
Mexico City, Mexico	300	2004–2006	Differential interferometry	Osmanoglu et al. (2011)
Murcia, Spain	35	2008–2009	differential interferometry	Herrera et al. (2010)
Phoenix-Scottsdale, Arizona, US	15	2004–2010	Differential interferometry	ADWR (2011)
Saga Plain, Japan	160	1994	Leveling	Miura et al. (1995)
Semarang, Indonesia	80	2007–2009	Differential interferometry	Lubis et al. (2011)
Tehran Basin, Iran	205–250	2004–2008	Differential interferometry	Dehghani et al. (2010)
Tokyo, Japan	40	1988–1997	?	Hayashia et al. (2009)
Toluca Valley, Mexico	90	2003–2008	Differential interferometry	Calderhead et al. (2010)
Yunlin, Republic of China	100	2002–2007	Leveling	Hung et al. (2010)

 DOI 10.1007/s10040-011-0775-5

although third order standards also have been used. First order class I leveling is double run and requires that the allowable discrepancy between section (backward and forward lines) misclosures does not exceed $3\sqrt{E}$ mm where E is the shortest one-way length of the section line in kilometers (Federal Geodetic Control Committee 1984, sect. 3.5, pp. 3–8). Second order class I leveling requires a closure error not to exceed $6\sqrt{E}$ mm and generally costs less per kilometer than first order class I surveys. Partly because of the difference in cost between first-order leveling and second-order leveling, it is common practice in resurveying a network in a subsiding area to select principal lines for first-order re-leveling and secondary lines for second-order re-leveling. It is extremely important that ties to "stable" ground, for example consolidated sediments or bedrock, be included in the first-order leveling.

Any procedures that reduce loop closing time are beneficial in order to minimize the effects of land-surface elevation changes occurring during the survey. The time of year when the leveling is done is important in a heavily pumped basin, for example, one where local annual fluctuations of hydraulic head are 10–30 m. Commonly drawdowns occur in the spring and summer and recoveries occur in the autumn and winter when withdrawal is less. Hence, applied stresses are much greater in the summer than in the winter, and the full annual compaction of the aquifer system may occur in 5–6 months. In such areas, leveling optimally is accomplished during or immediately following the period of recovering hydraulic heads when compaction and subsidence are minimal.

Global positioning system (GPS)

A revolution in surveying and measurement of crustal motion occurred in the early 1980s when tests of the satellite-based NAVSTAR global positioning system (GPS) showed that it was possible to obtain 1 part in 1 million precision between points spaced from 8 to more than 40 km apart. GPS uses signals from at least four Earth-orbiting satellites to determine approximate absolute (i.e. non-differential) positions of an autonomous receiver. For differential geodetic surveys GPS observations collected simultaneously at two receivers—one receiver may be a continuous global positioning system—CGPS station, for example CORS (continuously operating reference stations; see NOAA 2011) are used to compute a precise baseline between the receivers (in real time if appropriate communication exists between the two receivers). Given the known location of the CGPS (or base station), the 3D position of the roving receiver can be determined by adding the observed baseline vector to the known position. Since 17 July 1995, NAVSTAR GPS has been operational with a full constellation of 24 satellites, and in North America provides essentially continuous coverage with nominally at least six satellites in view at all times. The GPS satellites are referenced to the World Geodetic System of 1984 (WGS 84) ellipsoid. GPS positioning routinely determines ellipsoid heights (position above below the reference ellipsoid) and elevations (orthometric heights—distance between Earth's surface and the geoid, a reference surface which approximates mean sea level) are obtained from ellipsoid heights and geoid heights (difference between the reference ellipsoid and geoid). Guidelines for establishing GPS-derived ellipsoid heights at the 20- and 50-mm levels are described by Zilkoski et al. (1997) and guidelines for establishing GPS-derived orthometric heights are described by Zilkoski et al. (2008).

In land-subsidence and other crustal-motion surveys, the relative and absolute 3D positions of reference marks can be determined using GPS. Geodetic networks of reference marks can be surveyed and resurveyed in this fashion. Such a network, one of the first of its kind designed specifically to monitor land subsidence caused by groundwater extraction, was established in the Antelope Valley, Mojave Desert, California in 1992 (Fig. 2; Ikehara and Phillips 1994) to determine the subsidence of previously leveled bench marks and to enable precise measurement of points separated by tens of kilometers for future subsidence monitoring. Other large GPS-based geodetic networks for subsidence monitoring in the US have been established in Albuquerque, New Mexico (C. Heywood, US Geological Survey, personal communication, 2003); the Avra Valley and the Tucson basin, Arizona (Carruth et al. 2007); Houston-Galveston area, Texas (Zilkoski et al. 2003); Las Vegas, Nevada (Bell et al. 2002); the Lower Coachella Valley, California (Sneed and Brandt 2007); and the Sacramento-San Joaquin Delta, California (M. Ikehara, NOAA, personal communication, 2008). GPS surveying also is a versatile exploratory tool that can be used in rapid kinematic or rapid static mode to quickly and coarsely define subsidence regions, in order to site more precise, site-specific and time-continuous measurement devices such as recording extensometers, tiltmeters and CGPS.

One of the strengths of GPS is the ability to measure both horizontal and vertical movements. Subsidence and uplift associated with managed subsurface fluid production and storage practices is accompanied by measurable horizontal movements in the Earth's crust. If the points are on the margin of a subsidence/uplift feature, then the ratio of vertical to horizontal motion may be nearly 1:1 (Bawden et al. 2001). For example, in the San Gabriel Valley in southern California, groundwater pumping pulled nearby CORS inward toward the region of maximum drawdown (Fig. 3), and record rainfall in the same region in the winter-spring 2005 produced more than 4 cm of uplift with greater than 1 cm of radial outward motion of the nearby CORS (King et al. 2007). Burbey et al. (2006) used vertical and horizontal GPS measurements during a 60-day aquifer test to show that a single value of lateral permeability anisotropy for the aquifer rather than a trending anisotropy can yield different angles of deformation (combinations of radial and tangential) as a function of radial distance from the pumping well.

Tripod LiDAR

Ground-based Tripod Light Detection and Ranging (T-LiDAR) is a portable remote sensing instrument that uses

 DOI 10.1007/s10040-011-0775-5

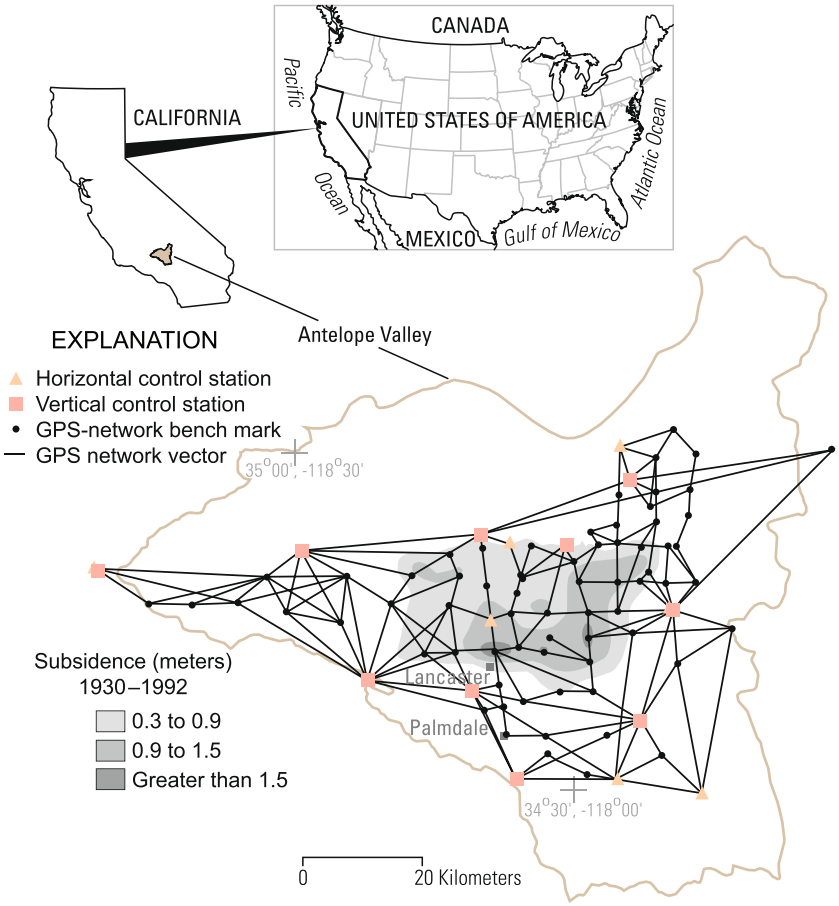

Fig. 2 Geodetic network used to measure historical subsidence in 1992 in Antelope Valley, Mojave Desert, California. Results from the geodetic surveys and conventional leveling surveys showed a maximum subsidence of about 2 m; more than 500 km^2 had subsided more than 0.6 m since about 1930 (Ikehara and Phillips 1994). Modified from Galloway et al. (1999; p. 145)

an infrared laser to scan the landscape and generate very detailed (centimeter to sub-centimeter) and accurate 3D digital models of the scanned target at distances from 2 to 2,000 m (G. Bawden, US Geological Survey, personal communication, 2010). More than 7 million point-position measurements per hour can be made depending upon the particular T-LiDAR system; scan rates, data densities, and point positional errors vary among the different systems. A full 3D image is obtained by scanning a target from multiple directions to characterize all sides of the target area and to minimize shadowing. T-LiDAR scans imaged from different vantage points are aligned and combined through an algorithm that computes a best-fit surface through the individual points in each scan and then minimizes the misfit between common surfaces in each scan.

Changes in the position of the land surface or a structural feature can be obtained through differencing of precisely aligned T-LiDAR images collected at different times, known as Differential LiDAR (Dif-LiDAR). There are two approaches for Dif-LiDAR analysis: absolute and relative. Absolute Dif-LiDAR measures land-surface change by differencing two LiDAR datasets that are georeferenced using the GPS. This approach produces the best information of land-surface change, but requires additional field equipment and time for GPS data collection and processing and may be unnecessary for some scientific applications. Alternatively, relative Dif-LiDAR applies the same best-fit surface-matching algorithm used in the alignment of an individual scan to common 'stable' regions outside of the area of interest that is changing. This approach is ideal for resolving very detailed spatial changes within a well-defined deformation zone or imaging change in a subset of a larger dataset where absolute positioning is not required. For example Dif-LiDAR could be used to measure 3D movement of infrastructure across deforming boundaries such as ground failures associated with aquifer-system compaction (Densmore et al. 2010). Dif-LiDAR can resolve the relative 3D displacement field, rotation, localized tilt, and translation within the scanned region, but requires GPS ground control to uniquely measure these parameters for the data block as a whole and to reference the measurements to a global reference frame. T-LiDAR is an ideal technique for measuring spatial and temporal changes in regions that are actively deforming, but the technique may be too labor intensive for characterizing subsidence features at scales greater than a few square kilometers.

Extensometry

Vertical borehole extensometers are used to measure the continuous change in vertical distance in the interval

 DOI 10.1007/s10040-011-0775-5

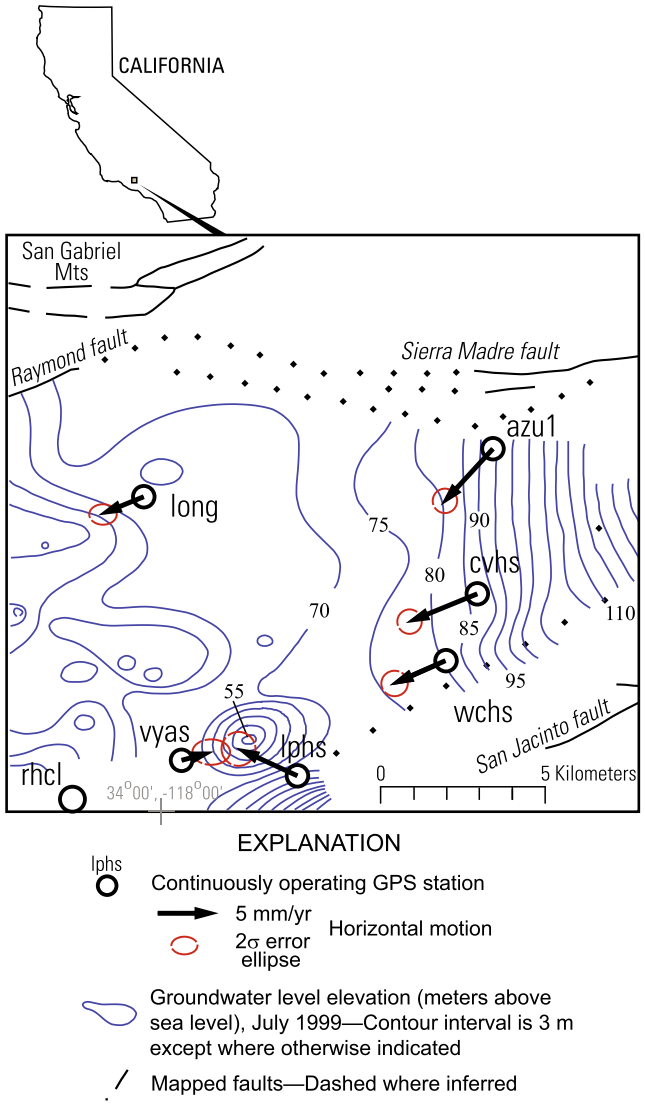

Fig. 3 Horizontal GPS displacement vectors for the Upper San Gabriel Valley, California. Groundwater levels in the valley declined about 3.5 m between May and October 1999 corresponding with approximately 12 mm of land subsidence (Bawden 2002). The neighboring continuously operating reference stations (CORS) *vyas* and *lphs* are pulled inward towards the zone of maximum subsidence which generally corresponds with the drawdown cone. The generally southwest-trending horizontal motion of the other CORS during this period is attributed to regional tectonic processes (Bawden et al. 2001). Modified from G. Bawden, US Geological Survey, personal communication, 2008)

between the land surface and a reference point or "subsurface bench mark" at the bottom of a deep borehole (Lofgren 1969; Riley 1986). If the subsurface bench mark is established below the base of the compacting aquifer system the extensometer can be used as the stable reference or starting point for local geodetic surveys. The deformation history generated by a borehole extensometer provides the basis for stress-strain analysis and modeling that constrains the material properties governing compaction of the aquifer system (see section Analysis and simulation).

Several types of early borehole extensometer designs are presented in Poland (1984). The anchored cable and pipe (free standing and counterweighted) extensometers have been used widely in a number of successful subsidence investigations. More recently, dual-stage counterweighted pipe extensometers (Fig. 4) have been used to measure compaction simultaneously in two depth intervals (e.g., Heywood 1993; Metzger et al. 2002; Wildermuth Environmental, Inc. 2006). Counterweighted pipe extensometers are capable of measurement resolutions of 0.01–0.1 mm (Riley 1969).

Multiple position borehole extensometers (MPBXs) that incorporate markers anchored to the formation borehole have been used effectively to monitor subsidence caused by groundwater extraction. Magnetic markers have been used in the Republic of China (ROC; Liu et al. 2004; Hwang et al. 2008) to compute vertical displacements in boreholes using repeat borehole logging with magnetic sensors on calibrated lines or tapes to measure temporal changes in marker positions. This method is capable of monitoring ten to several tens of marker positions in a single borehole at measurement resolutions of about 1–2 mm over depths of several hundred meters. The magnetic marker technique used in the ROC studies suggest that despite its poorer measurement resolution versus the counter-weighted pipe extensometer, this technique is suitable for monitoring seasonal and interannual inelastic and elastic deformation in many vertical intervals, and can be used to compute material properties based on the observed stress-strain behavior in portions of the aquifer systems undergoing sufficient deformation. Recent developments include fiber-optic sensors deployed in boreholes at multiple depths to measure compaction accompanying the extraction of natural gas dissolved in groundwater (Kunisue and Kokubo 2010). More applications of these techniques are warranted in many subsidence affected aquifer systems.

Several kinds of horizontal extensometers are used to measure differential horizontal ground motion at earth fissures caused by changes in groundwater levels (Carpenter 1993). Buried horizontal extensometers constructed of quartz tubes or invar wires are useful when precise, continuous measurements are required on a scale of 3–30 m. Tape extensometers measure changes across inter-monument distances as much as 30 m with repeatability of approximately 0.3 mm. The tape extensometer is used in conjunction with geodetic monuments specially equipped with ball-bearing instrument mounts, which can serve as both horizontal and vertical control points. Arrays or lines of monuments can be extended for arbitrary distances, usually in the range of 60–180 m.

Remotely sensed geodetic surveys and techniques

Airborne and space-based geodetic techniques that can measure changes in the land-surface position have significantly advanced over the past two decades with the development of satellite-borne differential interferometric synthetic aperture radar (InSAR) and airborne LiDAR techniques. The InSAR techniques can measure sub-centimeter ground displacements at high spatial detail

 DOI 10.1007/s10040-011-0775-5

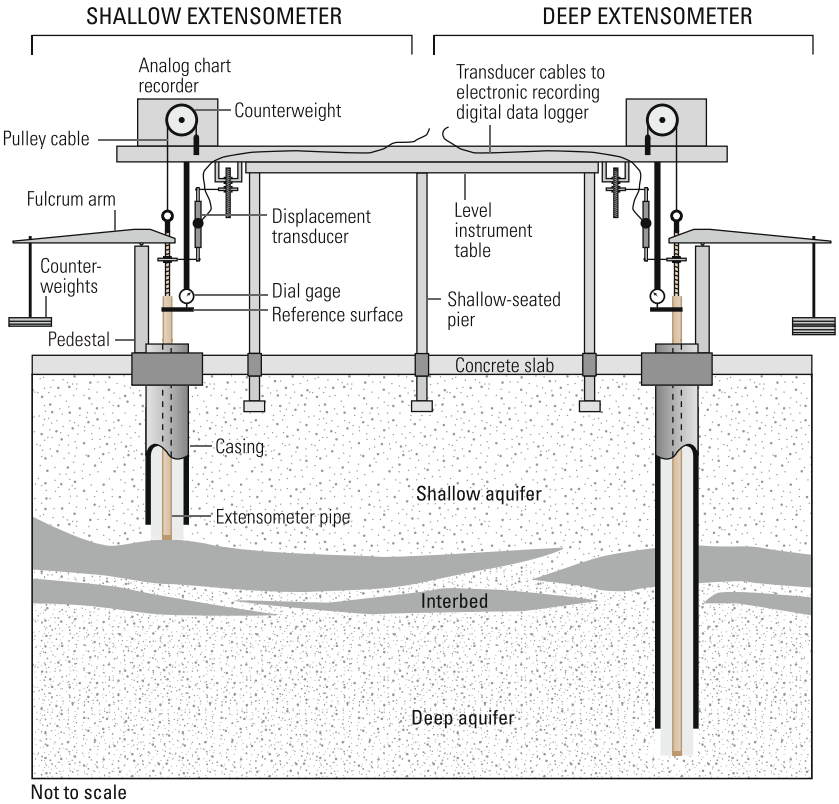

Fig. 4 Schematic of counter-weighted, two-stage, borehole pipe extensometer, Lancaster, California. The extensometer measures vertical displacement in two depth intervals in the aquifer system. The displacement is measured as movement of the pipe relative to the reference table and reflects shortening (subsidence) or lengthening (uplift) of the distance between the shallow-seated piers and the anchor depths of the pipe extensometers. Modified from Galloway et al. (1999, p. 146)

(10–100 m resolution) over regions spanning 10^4–10^5 km^2, but are limited to measuring changes in the line-of-sight distance between the ground and satellite, which are most sensitive to vertical motion if the radar look angle is less than 45° from the vertical. LiDAR imagery can be used to map larger-scale deformations using repeat airborne LiDAR techniques. The LiDAR discussed here for detecting surface elevation change is the 'spot comparison method'. An alternative processing technique that focuses on the shape of LiDAR multi-modal waveforms using the 'return pulse correlation' method (Hofton and Blair 2002) has advantages for detecting surface elevation change in vegetated areas and is not discussed here.

InSAR

Satellite InSAR is ideally suited to measure the spatial extent and magnitude of surface deformation associated with aquifer-system compaction. Two classes of InSAR techniques—firstly, single interferometric processing or conventional, coherent techniques, referred to here as conventional InSAR and secondly, multi-interferometric processing techniques such as the persistent-scatterer interferometry (PSI) and small baseline subset (SBAS) techniques, are used to map, monitor, and analyze subsidence. By identifying specific areas of deformation within broader regions of interest, InSAR also can be used to site and coordinate other local and regional-scale subsidence monitoring. For many areas, a substantial satellite synthetic aperture radar (SAR) data archive exists for the period 1991–present (ENVISAT; ERS-1, 2; JERS-1; Radarsat-1, 2). The conventional InSAR and PSI techniques have been most widely applied and are discussed in more detail in the following.

The spatial and temporal coverage of satellite SAR data depends on the SAR platform (Lu et al. 2010). Early spaceborne systems (ERS-1, ERS-2, and JERS-1) are of the strip-mode type, in which the radar look angle is fixed and the antenna footprint covers a relatively narrow strip (~50–100-km wide swath) on the surface to one side of the orbit track (cross-track direction). The new generation of SAR satellite platforms (Envisat, RADARSAT-1, and ALOS, and future systems) is capable of acquiring images in both strip mode and scan mode. A scan-mode SAR (ScanSAR) can periodically sweep the antenna look angle to image neighboring sub-swaths in the cross-track direction, thereby increasing the width of the image swath to as much as 400–500 km. Strip-mode SAR can only acquire images suitable for InSAR at the frequency of the satellite repeat orbit (46 days for ALOS; 44 days for JERS-1; 35 days for ERS-1, ERS-2 and Envisat; 24 days for RADARSAT-1 and RADARSAT-2; and 11 days for TerraSAR-X). ScanSAR can acquire more frequent observations suitable for InSAR analysis for a given study area than is possible with strip-mode SAR, and can signifi-

 DOI 10.1007/s10040-011-0775-5

cantly improve the temporal resolution of deformation mapping, albeit at the expense of some loss in spatial resolution (Guarnieri and Rocca 1999; Holzner and Bamler 2002). For example, at 45° latitude, Envisat can acquire 15 ScanSAR images of a target area that can be combined to produce time-sequential interferograms with a temporal resolution of 3 days, compared with 35 days for the same target area when Envisat is operating in strip mode. Thus, ScanSAR InSAR potentially is suitable for monitoring transient aquifer-system deformation associated with sub-weekly to weekly groundwater discharge and recharge cycles.

InSAR uses radar signals to measure deformation of the Earth's crust in high spatial detail and high measurement resolution. InSAR can provide millions of data points in a large region (10^4–10^5 km^2/scene) and often is less expensive than obtaining sparse point measurements from labor-intensive spirit-leveling and GPS surveys. Geophysical applications of InSAR take advantage of the phase component of reflected radar signals to measure apparent changes in the line-of-sight (range) distance of the land surface (Gabriel et al. 1989; Massonnet and Feigl 1998). For landscapes with relatively stable radar reflectors (such as buildings or other engineered structures, or undisturbed rocks and ground surfaces) over a period of time, it is possible to make high-precision measurements of the change in the position of the reflectors by subtracting or "interfering" two radar scans made of the same area at different times; the resulting InSAR image is called an interferogram. The size of a picture element (pixel) on a typical interferogram may be as small as 100 m^2 or as large as tens of thousands m^2, depending on the SAR platform, on the mode of SAR acquisition (strip mode versus scan mode) and on how the interferogram is processed.

Under ideal conditions, it is possible to resolve georeferenced changes in range distance between the ground and satellite, on the order of 10 mm or less at the scale of 1 pixel. The component of displacement measured using InSAR principally is vertical for past and current SAR systems and depends on the look angle of the sensor. Since 1998, conventional InSAR has been used widely to map spatially detailed ground-surface deformations associated with groundwater pumping (e.g., Galloway et al. 1998; Amelung et al. 1999; Bawden et al. 2001; Hoffmann et al. 2001; Bell et al. 2002; Hoffmann et al. 2003a; Schmidt and Bürgmann 2003; Chatterjee et al. 2006; Pavelko et al. 2006; Sneed and Brandt 2007; Anderssohn et al. 2008; Hung et al. 2010; Calderhead et al. 2010; Wisely and Schmidt 2010; Lubis et al. 2011). Figure 5a and b show a conventional InSAR-derived subsidence map and profiles for the Las Vegas Valley, Nevada compared to historical terrestrial geodetic measurements. Hydrogeologic applications of InSAR were reviewed by Galloway and Hoffmann (2007).

Persistent (also known as permanent) scatterer interferometry (PSI) uses a different approach than conventional InSAR for processing SAR imagery, and has been shown to overcome some of the limitations of the conventional InSAR technique. PSI involves the processing of numerous, typically 25 or more, interferograms to identify a network of persistent, temporally stable, highly reflective ground features—permanent scatterers (Ferretti et al. 2000, 2001; Werner et al. 2003). These scatterers typically are cultural features of the developed landscape such as buildings, utility poles, and roadways. The time-series phase measurements for each scatterer are extracted by estimating a predefined displacement model (typically a linear, constant-rate model) to provide interpolated maps of average annual displacements, or the displacement history, up to the length of a SAR data archive, of each individual scatterer, thus providing a "virtual" GPS network with "instant" history. By focusing on temporally stable targets in the image, temporal decorrelation is avoided or strongly reduced. Furthermore, most of the strong and stable reflectors identified represent small individual scattering elements. For this type of scatterer though, a larger fraction of the reflected energy remains coherent for larger interferometric baselines, allowing a larger set of SAR scenes to be used in PSI analysis than can be used in InSAR analysis. The large number of observations available in a typical SAR data set used in a PSI analysis supports a statistical analysis of the observed phase histories in space and time, and depending on the characteristics of the displacements, it often is possible to separate the phase differences caused by atmospheric variations and uncompensated topography from those due to surface displacements. The theoretical limit of the PSI technique is 1–2 mm in radar-range displacement (Ferretti et al. 2000).

PSI has been applied primarily in urban environments, where the density of stable scatterers typically is quite high (as many as a few hundred per square kilometer). Over natural terrain, the scarcity of stable targets severely limits PSI's successful application. A small number of investigations have demonstrated a successful application of PSI in "rural" terrain (Usai 2001; Kircher 2004). However, the investigations in the Netherlands and western Germany used stable targets such as houses and other manmade features that were present in sufficient numbers. Hooper et al. (2004, 2007) have proposed a modified algorithm (STaMPS) for natural terrain, but this has been demonstrated for relatively dry conditions and it is questionable whether their approach will work over agricultural areas prone to temporal decorrelation owing to variable moisture and crop conditions.

A potentially important limitation of PSI, particularly where scatterer density is small and displacement magnitudes are large, is the necessity to determine a motion model a priori, that is used to resolve phase ambiguities. Another limitation of PSI is the difficulty identifying stable targets in rural and agricultural areas. Consequently, the majority of PSI applications have focused on urban areas—for example, Paris, France (Fruneau and Sarti 2000); San Francisco Bay Area, California, US (Ferretti et al. 2004); Bangkok, Thailand (Worawattanamateekul et al. 2004); Phoenix, Arizona, US (Beaver et al. 2005);

 DOI 10.1007/s10040-011-0775-5

Arno River Basin-Florence, Italy (Canuti et al. 2005); Berlin, Germany (Kampes 2005); Las Vegas, Nevada, US (Kampes 2005; Bell et al. 2008); Murcia, Spain (Herrera et al. 2010) and Mexico City, Mexico (Osmanoglu et al. 2011). Figure 5c and d show a PSI-derived displacement velocity map for a portion of the Las Vegas Valley, Nevada, US and a compaction time series derived from PSI target DW197 near the Lorenzi extensometer compared to compaction measured by the borehole extensometer. The STaMPS algorithm overcomes some of the limitations of the PSI technique—fewer interferograms are needed, and an a priori deformation model is not needed (Hooper et al. 2007).

LiDAR

Airborne LiDAR is capable of rapidly and accurately collecting high-resolution elevation data in flat terrain with 9.1–18.2-cm vertical accuracies for high-grade commercial airborne LiDAR data (American Society of Photogrammetry and Remote Sensing 2004). Repeat airborne LiDAR imagery can be used to map large-scale deformation. Movements greater than 0.36–0.73 m are needed between LiDAR surveys to resolve land-surface motion with most high-grade airborne LiDAR, and this limits its use for many aquifer-system compaction related subsidence cases.

Analysis and simulation

The analysis and simulation of land subsidence accompanying deformation of aquifer systems owing to groundwater extraction typically is applied to unconsolidated alluvial or basin-fill aquifer systems comprising aquifers and aquitards. It is in these types of hydrogeologic settings that aquifer-system compaction causes significant and extensive land subsidence. The aquitards include the spectrum of low-permeability, thick and thin fine-grained deposits—discontinuous interbeds within the aquifers to laterally extensive confining units separating individual aquifers in the aquifer system. The interbeds and confining units are much less permeable than the hydraulically interconnected coarse-grained deposits constituting a single aquifer. By virtue of their limited lateral extent and typically smaller thickness the interbeds are conceptually distinct from the confining units (Fig. 6).

Various approaches to analyzing and modeling deformation of aquifer systems follow from the basic relations between head, stress, compressibility, and groundwater flow. Analysis and simulation of aquifer-system compaction have been addressed primarily using two approaches—one based on conventional groundwater flow theory (Jacob 1940, 1950) and one based on linear poroelasticity theory (Biot 1941). The former approach is a special case of the latter, and both approaches are based on the *Principle of Effective Stress* (Terzaghi 1923, 1925) which, assuming incompressible solid grains, can be expressed in terms of stress tensors as:

$$\sigma'_{ij} = \sigma_{ij} - \delta_{ij} p, \tag{1}$$

or in expanded form

$$\begin{vmatrix} \sigma'_{xx} & \sigma'_{xy} & \sigma'_{xz} \\ \sigma'_{yx} & \sigma'_{yy} & \sigma'_{yz} \\ \sigma'_{zx} & \sigma'_{zy} & \sigma'_{zz} \end{vmatrix} = \begin{vmatrix} \sigma_{xx} & \sigma_{xy} & \sigma_{xz} \\ \sigma_{yx} & \sigma_{yy} & \sigma_{yz} \\ \sigma_{zx} & \sigma_{zy} & \sigma_{zz} \end{vmatrix} - \begin{vmatrix} p & 0 & 0 \\ 0 & p & 0 \\ 0 & 0 & p \end{vmatrix},$$

where p is pore-fluid pressure, $\sigma_{ij'}$ and σ_{ij} are components of the effective stress and total stress tensors of order two, respectively, i and j for i=1–3 and j=1–3, represent the Cartesian coordinates x, y and z, respectively, and δ_{ij} is the Kronecker delta, where $\delta_{ij} = \begin{cases} 1, if\ i = j \\ 0, if\ i \neq j \end{cases}$. For a Newtonian fluid such as groundwater, the fluid cannot sustain shear stress, and therefore the off-diagonal components of the effective and total stress tensors are equal.

Equation 1 shows that changes in the effective stress can result from changes in the total stress or changes in pore-fluid pressure. The total stress is controlled by the geostatic stress (overburden load) of the overlying saturated and unsaturated sediments, tectonic stresses, and other factors such as topography and glacial history. If the aquitards are close to horizontal and are laterally extensive with respect to their thickness, the changes in pore-fluid pressure gradients within the interbeds will be close to vertical. If one further assumes that the resulting strains also are close to vertical (zz), a one-dimensional (1D) form of Eq. 1 becomes

$$\sigma'_{zz} = \sigma_{zz} - p, \tag{2}$$

where σ'_{zz} and σ_{zz} are the vertical effective stress and total stress, respectively. For the case where the total stress remains constant in time the change in effective stress is equal in magnitude and opposite in sense to the change in pore-fluid pressure:

$$\Delta\sigma'_{zz} = -\Delta p,\ for\ \Delta\sigma_{zz} = 0. \tag{3}$$

The chief difference between the two approaches is the treatment of the deformation of the skeletal matrix. Conventional groundwater flow theory describes only the vertical deformation of the matrix (assumes no horizontal deformation), whereas poroelasticity theory describes the 3D deformation of the matrix. Both approaches describe a coupled relation between fluid flow, effective stress and deformation of the aquifer system, but poroelasticity theory more rigorously couples fluid flow and deformation, and therefore is more physically realistic albeit more complex.

 DOI 10.1007/s10040-011-0775-5

Aquitard drainage model

The origins of the aquitard drainage model are attributed (Riley 1998) to pioneering works by Terzaghi (1923, 1925) on the consolidation of drained and undrained saturated clays and by Meinzer (Meinzer and Hard 1925; Meinzer 1928) who recognized that aquifer-system compaction is necessary to account for the amounts of water produced from aquifers, although he did not ascribe the deformation to aquitards. Tolman and Poland (1940) suggested that subsidence caused by groundwater extraction in the Santa Clara Valley, California was caused primarily by the largely non-recoverable compaction of slow-draining aquitards within the confined aquifer system, marking the conceptual birth of the aquitard drainage model. Riley (1969) quantitatively applied Terzaghi's (1923, 1925) theory of 1D vertical consolidation to the model. This concept has formed the theoretical basis of many successful subsidence investigations associated with depressuring of porous media (see Helm 1984a; Holzer 1998; Riley 1998). The aquitard drainage model is based on conventional groundwater flow theory and two principles of consolidation (Terzaghi 1923, 1925)—the Principle of effective stress (Eq. 2), and the Theory of hydrodynamic gag—describing the relations between fluid pressure, intergranular stress and fluid flow.

The standard diffusion equation for 3D transient groundwater flow can be expressed by

$$\nabla^2 h = \frac{\partial^2 h}{\partial x^2} + \frac{\partial^2 h}{\partial y^2} + \frac{\partial^2 h}{\partial z^2} = \frac{Ss}{K}\frac{\partial h}{\partial t}, \tag{4}$$

where

h is hydraulic head
S_s is specific storage, and
K is hydraulic conductivity.

The specific storage defined by Jacob (1940) assumes the storage changes are proportional to head, the solid grains are incompressible, and that only vertical deformation can occur (Cooper 1966):

$$Ss = \rho_w g(\overline{\alpha} + n\beta_w), \tag{5}$$

or expressed another way (Riley 1969),

$$Ss = Ss_k + Ss_w \tag{6}$$

where

$\overline{\alpha}$ is the vertical matrix or skeletal compressibility,
β_w is the compressibility of water
n is porosity
ρ_w is the density of water
g is the gravitational acceleration
Ss_k is the skeletal specific storage, $Ss_k = \rho_w g\alpha$, and
S_{s_w} is the water specific storage, $S_{s_w} = \rho_w gn\beta_w$.

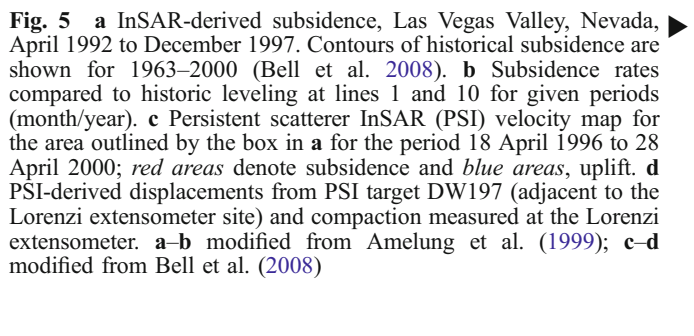

Fig. 5 **a** InSAR-derived subsidence, Las Vegas Valley, Nevada, April 1992 to December 1997. Contours of historical subsidence are shown for 1963–2000 (Bell et al. 2008). **b** Subsidence rates compared to historic leveling at lines 1 and 10 for given periods (month/year). **c** Persistent scatterer InSAR (PSI) velocity map for the area outlined by the box in **a** for the period 18 April 1996 to 28 April 2000; *red areas* denote subsidence and *blue areas*, uplift. **d** PSI-derived displacements from PSI target DW197 (adjacent to the Lorenzi extensometer site) and compaction measured at the Lorenzi extensometer. **a**–**b** modified from Amelung et al. (1999); **c**–**d** modified from Bell et al. (2008)

The 1D skeletal compressibility,α, can be defined based on the ratio of vertical strain to vertical effective stress as

$$\overline{\alpha} = \frac{\frac{\Delta\overline{b}}{\overline{b}_0}}{\Delta\sigma'_{zz}} \tag{7}$$

where $\Delta\overline{b} = \overline{b}_0 - \overline{b}$ is the change in thickness of a control volume with initial thickness $b_0$of a deformable geologic unit. Note, both compaction and compressive stress are defined as positive values in this formulation. This is the matrix compressibility used in standard formulations for transient saturated groundwater flow (Jacob 1940, 1950). The vertical strain also can be expressed in terms of void ratio, e by $\frac{\Delta e}{1+e_0}$ where $\Delta e = e - e_0$ and e_0 are the change in void ratio and the initial void ratio, respectively. Thus, the skeletal specific storage in Eq. 6 can be expressed as

$$S_{s_k} = \frac{\Delta b\rho_w g}{b_0\Delta\sigma'_{zz}} = \frac{-\Delta e\rho_w g}{(1+e_0)\Delta\sigma'_{zz}} \tag{8}$$

Two skeletal specific storages can be further defined: (1) Ss_{ke} for the elastic range of stress where $\sigma'_{zz} \le \sigma'_{zz_{max}}$(the previous maximum effective stress); and (2) Ss_{kv} for the virgin or inelastic range of stress where $\sigma'_{zz} > \sigma'_{zz_{max}}$. For effective stress less than the previous maximum effective stress (preconsolidation stress threshold), the compaction or expansion of both aquitards and aquifers is approximately elastic—that is, approximately proportional to the change in effective stress over a moderate range in stress, and fully recoverable if the stress reverts to the initial condition. For effective stress greater than the preconsolidation stress threshold, the "virgin" compaction of aquitards is chiefly inelastic—that is, not fully recoverable upon decrease in effective stress. This virgin compaction includes a recoverable elastic component that is small when compared to the inelastic component. The virgin compaction is roughly proportional to the change in logarithm of effective stress. In contrast to aquitards, typically the compaction of aquifers is chiefly elastic but it may include a small inelastic component. In poorly sorted and angular sands, and especially in micaceous sands, the inelastic component may dominate.

The aquitard drainage model is based on the generality that when aquifer systems are developed, the release of water from storage in aquitards provides water and aquifers transmit it to wells (e.g. see Konikow and Neuzil 2007)—

DOI 10.1007/s10040-011-0775-5

a

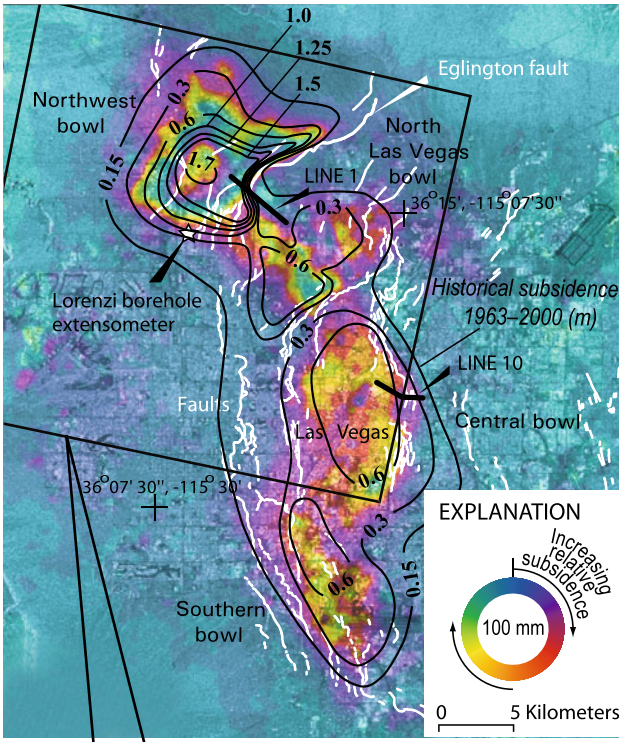

b

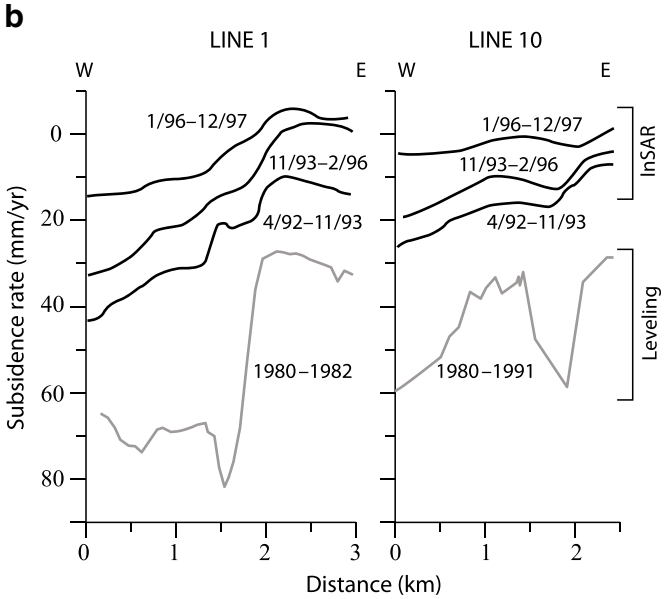

c

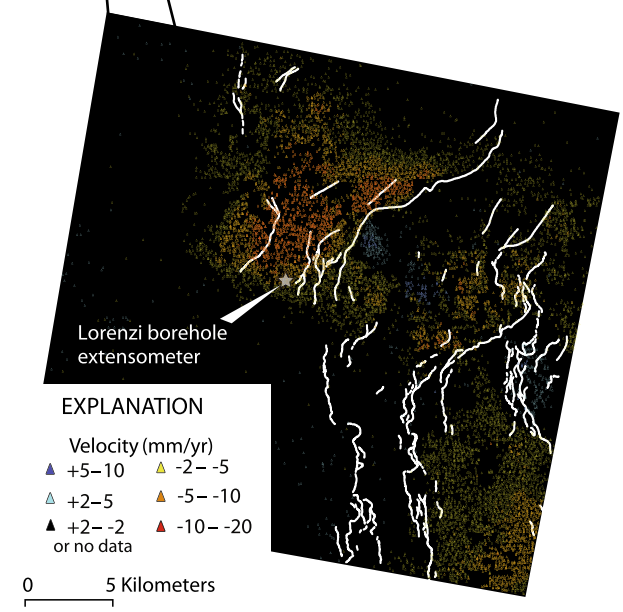

d

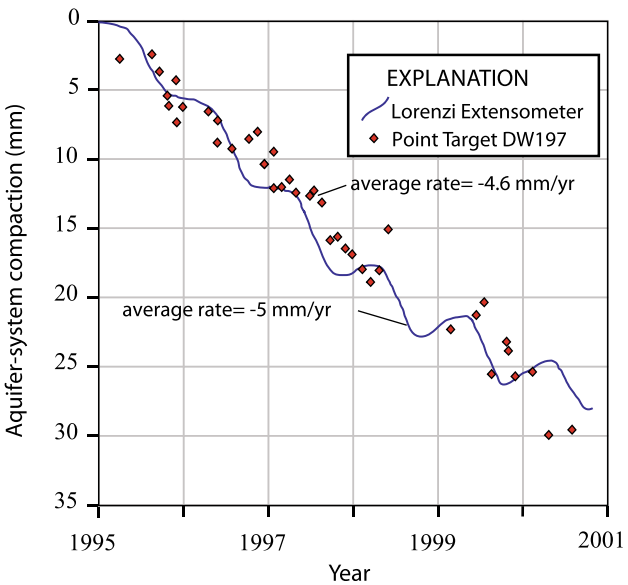

DOI 10.1007/s10040-011-0775-5

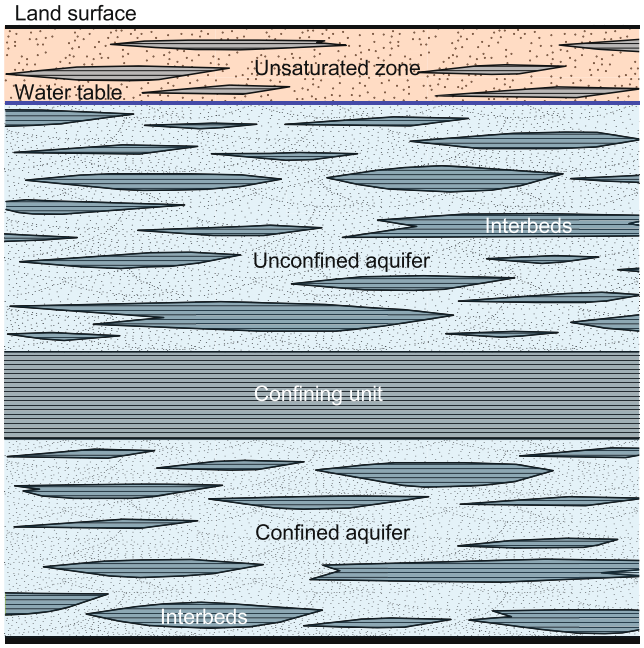

Fig. 6 Schematic vertical section of an aquifer system comprising unconsolidated relatively coarse- and fine-grained deposits. The relatively coarse-grained deposits constitute the aquifers. The relatively fine-grained units constitute the aquitards—confining unit and interbeds. Modified from Leake and Galloway (2007, Fig. 1)

that flow in aquitards principally is vertical owing to the large contrast in hydraulic conductivity between aquitards and aquifers (generally greater than two orders of magnitude). As such, a 1D form of Eq. 4 can be used to describe groundwater flow in aquitards:

$$\frac{\partial^2 h}{\partial z^2} = \frac{Ss'_k}{K'_z}\frac{\partial h}{\partial t} \tag{9}$$

where $'$ denotes material properties of the aquitard, and

$K_{z'}$ is the vertical hydraulic conductivity, and
Ss'_k is the skeletal specific storage (Eq. 6), recognizing that for aquitards in unconsolidated alluvial aquifer systems $\alpha' \gg \beta_w$.

Terzaghi (1923, 1925), using a nondimensional form of Eq. 9, showed that consolidation is essentially complete when the dimensionless time (T_D) is unity, leading to the notion of a time constant (τ') or characteristic time where

$$T_D = \frac{t}{\tau'} \tag{10}$$

Terzaghi (1923, 1925) developed an analytical solution for an equivalent of Eq. 9 to simulate the equilibration of head (equivalent pore-fluid pressure) in a saturated clay sample with uniform initial head where only vertical flow is permitted, in response to a specified instantaneous step change in head at the top and bottom of the sample. This process describes the *theory of hydrodynamic lag (consolidation)* which was extended to the analysis of aquitard drainage (Riley 1969), and subsequently to the simulation of aquitard drainage (Helm 1975, 1976).

The theory describes the delay in draining aquitards when heads are lowered in adjacent aquifers, as well as any residual compaction of the aquitards that may continue long after the heads are initially lowered. The application of the hydrodynamic consolidation theory of soil mechanics to aquifer-system compaction has been summarized lucidly by Riley (1969, pp. 425–426).

The time constant τ' for a doubly draining aquitard is (Riley 1969; Helm 1975, p. 470):

$$\tau' = \frac{Ss'\left(\frac{b'}{2}\right)^2}{K'_z} \tag{11}$$

where b' is the thickness of the aquitard, $S'_{s_l} = S'_{s_e} = S'_{s_{ke}} + S'_{s_w}$ for the elastic range of stress, where Ss'_e and Ss'_{ke} are the elastic specific storage and elastic skeletal specific storage, respectively, and $S'_s = Ss'_v \cong Ss'_{kv}$ for the inelastic range of stress, where Ss'_v and Ss'_{kv} are the inelastic specific storage and inelastic skeletal specific storage, respectively, and τ' is the time, t in Eq. 10, required to attain about 93 percent of the ultimate consolidation.

As implied by the two definitions given above for Ss'_k (one for elastic and one for inelastic stress), time constants can be computed for both the elastic (τ'_e) and inelastic (τ'_v) stress ranges. Detailed development of the hydrodynamic consolidation theory for soils summarized above for aquitards is given in Scott (1963, pp. 162–197).

The use of numerical models to simulate and predict aquifer-system compaction based on the aquitard-drainage model were developed during the last three decades of the 20th century with the advent of digital computers capable of numerically solving partial differential equations rendered as large systems of algebraic equations. Methods to simulate compaction in aquifer systems based on the aquitard drainage model were developed by Helm (1972, 1975, 1976), Witherspoon and Freeze (1972), Gambolati and Freeze (1973), Narasimhan and Witherspoon (1977), and Neuman et al. (1982).

The numerical formulation of the aquitard-drainage model led directly to important simulation tools and powerful predictive techniques for land subsidence caused by water-level fluctuations within a confined aquifer system. The 1D (vertical) model (COMPAC) presented by Helm (1984b, 1986) computes compaction caused by specified water-level changes. This approach has been used widely to analyze compaction, estimate critical aquifer-system parameters, and predict future subsidence at borehole extensometer sites for which there are detailed records of water-level changes, compaction and (or) subsidence (e.g. Helm 1978, 1984b; Epstein 1987; Hanson 1989; Pope and Burbey 2003, 2004; Liu and Helm 2008a, b).

Other modeling efforts focused on incorporating subsidence calculations in widely used two-dimensional (2D) and 3D models of groundwater flow. Meyer and Carr (1979), Williamson et al. (1989), and Morgan and Dettinger (1996) modified and used finite-difference models to simulate groundwater flow and subsidence in

 DOI 10.1007/s10040-011-0775-5

the area of Houston, Texas; the Central Valley, California; and Las Vegas Valley, Nevada, respectively. Leake and Prudic (1991) developed the Interbed Storage Package, version 1 (IBS1), to simulate regional-scale compaction of interbeds within aquifers using the widely applied modular groundwater-flow model, MODFLOW (McDonald and Harbaugh 1988). IBS1 also can be used to simulate compaction of confining units if these units can be discretized into one or more model layers (Larson et al. 2001; Nishikawa et al. 2001). MODFLOW and the IBS1 Package have been used to simulate 3D regional groundwater flow and land subsidence (e.g., Hanson et al. 1990; Hanson and Benedict 1994; Galloway et al. 1998; Nishikawa et al. 2001; Kasmarek and Strom 2002; Hanson et al. 2003a, b; Leighton and Phillips 2003; Don et al. 2006), as well as 1D groundwater flow and compaction measured at borehole extensometer sites (Sneed and Galloway 2000; Pavelko 2003). The IBS1 formulation assumes that during one model time step, head changes in aquifer material are propagated throughout the entire thickness of compressible interbeds which implicity assumes that the interbeds are thin enough for heads to equilibrate with aquifer head changes during a single model time step. A similar approach to simulating regional subsidence and groundwater flow was implemented in HydroGeoSphere (Therrien et al. 2010) and applied to the Toluca Valley, Mexico (Calderhead et al. 2011).

To address time-dependent aquitard drainage, Leake (1990) developed the Interbed Storage Package, version 2 (IBS2). Later studies used IBS2 to investigate the potential effects of land subsidence in the presence of delay interbeds (e.g., Leake 1990, 1991; Wilson and Gorelick 1996). A similar approach was reported by Shearer (1998) to simulate groundwater flow and subsidence, accounting for the time-dependent drainage and compaction of thick clay units. The SUB Package (Hoffmann et al. 2003b) updates the functionality of IBS1 and IBS2 for MODFLOW-2000 (Harbaugh et al. 2000) and MODFLOW-2005 (Harbaugh 2005), and was used to simulate subsidence in California's Central Valley Aquifer (Faunt 2009).

The techniques presented in the preceding for simulating the aquitard drainage model are based on the assumption that total or geostatic stress is constant (Eq. 3), which is violated when heads in an unconfined aquifer are changed; thus, these techniques tend to overestimate subsidence in developed unconfined aquifers and any underlying confined aquifers. Originally developed by Leake (1991) as the IBS3 Package, the SUB-WT Package (Leake and Galloway 2007) for MODFLOW-2000, -2005 simulates geostatic stress as a function of water-table elevation and is useful for simulating subsidence in aquifer systems with shallow, unconfined aquifers. The SUB-WT Package also simulates stress-dependent changes in storage properties, as does the COMPAC model. Table 2 summarizes the principal capabilities of the MODFLOW-based subsidence packages and the COMPAC model.

Poroelasticity model

Unlike the approach taken in development of the aquitard drainage model using conventional groundwater flow equations and the 1D specific storage to account for vertical deformation of aquifer systems, poroelasticity theory describes the more fully coupled processes of groundwater flow and the 3D deformation of aquifer systems. The poroelasticity model can be used to simulate the 3D displacement of the aquifer system and land surface. Historically, horizontal strains (and displacements) in subsidence studies have been ignored for various reasons. Jacob (1940), for instance, ignored horizontal strains in the derivation of the storage coefficient for mathematical expediency, but never insinuated that such strains were negligible. Certainly, the exclusion of horizontal strain makes analytical calculations far more tractable. Perhaps a bigger reason why 1D vertical-displacement models have persisted is because many researchers argue that horizontal strains are much smaller than vertical strains in most subsidence investigations and can therefore be ignored. However, such arguments have been made without sufficient evidence for their exclusion. Wolff (1970) was perhaps the first to closely examine the role of horizontal strains during aquifer testing and concluded that they were indeed important noting a clearly defined zone of radial compression centered about the pumping well.

Biot (1941) developed 3D poroelasticity theory. The general theory accounts for compressible fluid, porous matrix and solid grains. However, similar to the development of the conventional groundwater flow equations, the presentation here assumes the solid grains are incompressible and follows the development presented by Verruijt (1969). The assumption of incompressible solid grains in studies of land subsidence is justified in most cases. Because the compressibility of individual solid grains is about 1–2 orders of magnitude smaller than that of pore water and 2–3 orders smaller than that of the porous skeleton, solid-grain compressibility is relatively negligible and generally ignored by hydrogeologists in the study of aquifer-system compaction.

Table 2 Principal features of the MODFLOW-based subsidence models—SUB and SUB-WT, and the COMPAC model

Simulation Feature	SUB	SUB-WT	COMPAC
3D (layers) groundwater flow and regional subsidence	⊕	⊕	
Variable geostatic loads		⊕	
Time-dependent (residual) compaction of interbeds	⊕		⊕
Time-dependent (residual) compaction of confining units	⊕	⊕	⊕
Stress-dependent storage properties of aquitards		⊕	⊕
Stress-dependent hydraulic conductivity of aquitards			S_{s_w}

 DOI 10.1007/s10040-011-0775-5

Transient groundwater flow that incorporates storage derived from volume deformation of the skeletal matrix can be expressed as

$$K\nabla^2 h = \rho_w g n \beta_w \frac{\partial h}{\partial t} + \frac{\partial}{\partial t} \times \left[\frac{\partial u_x}{\partial x} + \frac{\partial u_y}{\partial y} + \frac{\partial u_z}{\partial z}\right], \text{ or } K\nabla^2 h = S s_w \frac{\partial h}{\partial t} + \frac{\partial}{\partial t} \nabla \bullet u, \quad (12)$$

where

$u_{x,y,z}$ are the component displacements of the granular skeleton
u is a vector representing the displacement field of the granular skeleton, and
$\nabla \bullet u$ represents the volume strain of the skeletal matrix.

Equation 12 is one of many forms of the groundwater flow equation valid for volume deformation of the aquifer system. In many compacting basins where the matrix compressibility is large, the first term on the right hand side of Eq. 12 representing water compressibility often is ignored (Helm 1987) for mathematical expedience and tractability. In order to formulate a complete hydro-mechanically coupled solution equations relating the mechanical deformation of the skeletal matrix in terms of head and displacement are needed (Biot 1941):

$$\begin{aligned}
&(\lambda + G)\frac{\partial}{\partial x}\left[\frac{\partial u_x}{\partial x} + \frac{\partial u_y}{\partial y} + \frac{\partial u_z}{\partial z}\right] \\
&+ G\left[\frac{\partial^2 u_x}{\partial x^2} + \frac{\partial^2 u_x}{\partial y^2} + \frac{\partial^2 u_x}{\partial z^2}\right] - \rho_w g \frac{\partial h}{\partial x} \\
&= 0(\lambda + G)\frac{\partial}{\partial y}\left[\frac{\partial u_x}{\partial x} + \frac{\partial u_y}{\partial y} + \frac{\partial u_z}{\partial z}\right] \\
&+ G\left[\frac{\partial^2 u_y}{\partial x^2} + \frac{\partial^2 u_y}{\partial y^2} + \frac{\partial^2 u_y}{\partial z^2}\right] - \rho_w g \frac{\partial h}{\partial y} \\
&= 0(\lambda + G)\frac{\partial}{\partial z}\left[\frac{\partial u_x}{\partial x} + \frac{\partial u_y}{\partial y} + \frac{\partial u_z}{\partial z}\right] \\
&+ G\left[\frac{\partial^2 u_z}{\partial x^2} + \frac{\partial^2 u_z}{\partial y^2} + \frac{\partial^2 u_z}{\partial z^2}\right] - \rho_w g \frac{\partial h}{\partial z} \\
&= 0, \text{or}(\lambda + G)\nabla(\nabla \bullet u) + G\nabla^2 u - \rho_w g \nabla h \\
&= 0,
\end{aligned} \quad (13)$$

where

λ is one of Lame's constants, and
G is the rigidity or shear modulus.

The development of the set of Eq. (13) is described in more detail by others (including Wang 2000; Ingebritsen et al. 2006, pp. 52–54) and is based on force equilibrium (assuming no change in body force), the constitutive equations for a homogeneous medium and equations relating strain and displacement, assuming linear elasticity and incompressible solid grains. Taken together Eqs. 12 and 13 comprise four equations and four unknowns (h, u_x, u_y, u_z) that describe the poroelasticity relations, limited by the assumptions previously stated, needed to couple 3D groundwater flow and deformation in aquifer systems. The simultaneous solution of these equations is achieved using appropriate boundary and initial conditions, specified parameter values, and numerical methods to approximate the partial derivatives.

It is well known that the extraction of subsurface fluids causes 3D deformation of a pumped aquifer system, and there are several quantitative analyses of the phenomenon (Verruijt 1969; Sandhu 1979; Hsieh 1996; Burbey and Helm 1999; Burbey 2001a; Burbey 2005). As Hsieh (1996) notes, "Analysis of realistic aquifer settings generally requires a numerical poroelasticity model. This type of model is not well-known to most ground-water hydrologists." And, as others (Gambolati et al. 2000; Burbey 2001b) have shown, both approaches—conventional groundwater theory and linear poroelasticity—yield nearly identical head and volume-strain distributions and therefore, nearly identical volumes of water released from storage owing to subsidence. Minor differences in the transient behavior of horizontal surface ground displacements have been shown (Gambolati et al. 2000). However, the historical focus on groundwater quantity and secondarily regional head declines in developed groundwater basins, coupled with the paucity of regional horizontal-displacement measurements has led to wider application of analytical and numerical models based on the simpler conventional groundwater flow theory embodied in the aquitard drainage model. Nevertheless, shortcomings in the conventional approach exist (e.g., Burbey 2001a, b; 2002), especially in simulating the displacement field. The differences in the two approaches particularly are manifest near pumping centers and where heterogeneities in developed aquifer systems may contribute to large horizontal movements and hazards such as earth fissuring, movement of surface faults, damage to buildings and engineered conveyances (e.g., pipelines, drainageways, roadways, and canals/aqueducts). Burbey (2001b) showed that by ignoring horizontal strain, 1D subsidence models may overestimate vertical compaction or the specific storage used to calibrate to the observed compaction particularly near the pumping well where horizontal strains can be significant. The increasing capability to acquire 3D positional measurements using GPS is providing more information on horizontal movements at land surface and thereby insight, motivation and constraints for using poroelasticity models. For example, Burbey et al. (2006) and Burbey (2006) used horizontal and vertical GPS measurements during a 60-day aquifer test to calibrate a groundwater flow and deformation model with water-level measurements from only the pumping well. The nature of the horizontal deformation signal allowed them to identify a

 DOI 10.1007/s10040-011-0775-5

normal fault and to characterize the properties of the fault. These results reveal the potential importance and power of obtaining horizontal and vertical deformation measurements in the analysis of stressed aquifer systems. Water-level signals alone typically are inadequate for characterizing storage properties because small water-level changes generally are insensitive to storage changes. Conversely, even small storage changes often are reflected in the horizontal and vertical deformation signals (Burbey 2006).

Poroelasticity models based on numerical solution of Eqs. 12 and 13 have been used in several different hydrogeologic applications, a few of which are mentioned here. Finite-element solutions have been applied extensively in soil compaction and land subsidence analyses (Sandhu 1979). Hsieh (1996) used a 2D axisymmetric finite-element program (BIOT2D) to simulate deformation and deformation induced changes in hydraulic head including the Noordbergum reverse water-level effect attributed to local compression and transient increased pore-fluid pressure in an aquitard in response to pumping from an adjacent aquifer. Burbey and Helm (1999) implemented the granular displacement model (GDM) which uses an iterative approach at each time step to numerically solve for the displacement field which is then used to compute heads using MODFLOW (McDonald and Harbaugh 1988) which are then used to solve for the displacement field, and so on until convergence of both head and displacement is achieved. Coupling between Eqs. 12 and 13 in GDM is described as weak but stable and produces accurate results for flow-induced displacement that compare favorably with Hsieh's (1996) model (Burbey and Helm 1999). GDM was used to simulate displacement fields near low-permeability barriers (such as faults) in basin-fill deposits in Las Vegas Valley, Nevada and demonstrated that regional groundwater extractions can cause large horizontal strains near faults and likely play a key role in the development of earth fissures (Burbey 2002). Helm (1994) and Li (2007a, b, c) demonstrated horizontal transient movement of confined and unconfined aquifers with an analytical analysis of the velocity and displacement fields and showed that possible tensile stress due to groundwater discharge and recharge may occur and cause earth fissures along the boundary between the strain extension and compression zones near a pumping well. Kim and Parizek (1999) adeptly introduced deformation-dependent porosity and hydraulic conductivity into a Biot style poroelasticity code to reveal that deformation dependencies of the hydraulic properties induce nonlinear consolidation, which diverge from deformation patterns produced by mathematical models that use constant hydraulic parameters.

Other constitutive models: nonlinear poroelasticity and poroviscosity

In addition to the aquitard drainage and linear poroelastic models, other constitutive models have been introduced for investigation of land subsidence caused by groundwater withdrawals. Analytical solutions for nonlinear poroelastic models were developed for material displacement and velocity accompanying subsidence caused by artificial discharge and recharge (Li and Helm 2001a, b; Li 2000, 2003). The theory of poroviscosity also was introduced for the study of land subsidence (Helm 1998) to more adequately address the behavior of argillaceous material subjected to deformation caused by the flow of water through a saturated sedimentary material that can be described as a nonlinear viscous fluid (Jackson et al. 2004). The advantages of poroviscosity theory over the traditional aquitard drainage model or poroelasticity theory is that it incorporates the three continuous phases of material behavior into one unified time-dependent theory, something that poroelasticity theory must define as three separate physical processes which must be estimated in a linear fashion. These three transient processes are referred to as instantaneous (early time), primary consolidation (intermediate time) and secondary consolidation (late time) and often can be identified in laboratory consolidation tests. For example, Fig. 7 shows the results from a constant-load consolidation test (Taylor 1948) where these three processes can be readily observed as an initial strain (instantaneous) followed by primary consolidation and finally secondary compression. The latter process is identified as the portion of the curve that deviates from the tangent to the primary consolidation curve. Furthermore, the poroviscosity theory intrinsically allows for the transient behavior of porosity and hydraulic conductivity during consolidation, making it a powerful mathematical description of porous material. The models describe both the transient and dynamic (e.g., seismic) processes. The tangent line shown in Fig. 7 illustrates the linear approximation poroelasticity theory uses to approximate primary consolidation. Poroelasticity cannot intrinsically accommodate early time or late time consolidation.

Helm's (1998) 1D poroviscosity constitutive relation describing a laterally confined material undergoing axial deformation is

$$\begin{cases} \sigma' = \eta \dfrac{d\varepsilon}{dt} \\ \sigma' = \pm A \dfrac{d\eta}{dt} \end{cases} \tag{14}$$

where η is the dynamic viscosity, $\frac{d\eta}{dt}$ is the time rate of change of viscosity, $\frac{d\varepsilon}{dt}$ is the time rate of change of strain,

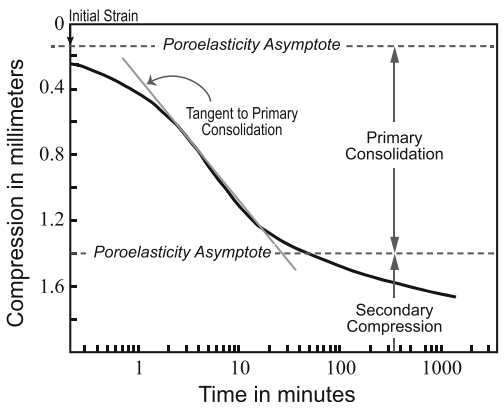

Fig. 7 One-dimensional consolidation test curve showing three independent physical processes—instantaneous strain (*initial*), *primary consolidation* (intermediate time) and *secondary compression* consolidation (late time). Modified from Taylor (1948)

 DOI 10.1007/s10040-011-0775-5

and A is a dimensionless poroviscous constitutive constant coefficient. The two expressions in Eq. 14 can be combined to form a single compact expression:

$$\frac{d\sigma'}{dt}\Big/\sigma' = \left(\frac{d^2\varepsilon}{dt^2}\Big/\frac{d\varepsilon}{dt}\right) + \left(\frac{d\varepsilon}{dt}/A\right) \tag{15}$$

where $\frac{d^2\varepsilon}{dt^2}$ is the time rate of change of $\frac{d\varepsilon}{dt}$. Equation 15 represents a powerful nonlinear expression that describes all three phases of observed compression (Fig. 7) and there is only one constant coefficient, A, that requires determination through laboratory testing (analogous to Young's modulus in poroelasticity theory). Equation 15 can be used to define the normal stress (the diagonal terms of Eq. 1) and the mean normal effective stress, σ'_m in terms of strain rates and dynamic viscosity. Darcy-Gersevenov law (Helm 1987) coupled with stress equilibrium and mass balance yield a governing equation in terms of the displacement field of solids and mean effective stress:

$$\frac{du}{dt} - \frac{K(3\lambda + 2G)}{3\rho_w g}\nabla(\nabla \bullet u) = q_b + \frac{K}{\rho_w g}\nabla\sigma_m \tag{16}$$

where $\mathbf{K}$ is the hydraulic conductivity matrix, σ_m is the mean normal stress, and $\mathbf{q}_b$ is the bulk flux defined as

$$q_b = v_s - K\nabla h \tag{17}$$

where $\mathbf{v}_s$ is the velocity of solids (skeletal matrix). The right-hand side of Eq. 16 represents a forcing function and can be used to account for various types of boundary conditions. Helm (1998) and Jackson et al. (2004) concluded that the right-hand side of Eq. 16 is negligible in 1D consolidation problems and can be ignored. Jackson (2005) developed a 1D poroviscosity model based on Eqs. 15 and 16 and incorporated this theory into COMPAC (Helm 1986).

Several analytic and numerical models of poroviscosity were established by Li and Helm (1995, 1997 and 1998) for 3D land movement. A complete description of the full development of both the 1D and 3D poroviscous theory can be found in Jeng (2005). Analytical solutions for the models of poroviscosity and elasto-viscosity were developed for subsidence with specified boundary conditions (Li and Helm 2000, 2001c). The incorporation of poroviscosity theory into numerical models holds great promise for accurately simulating observed deformational behavior in heavily pumped basins where subsidence of fine-grained deposits is problematic. One-dimensional analytical (Helm 1998) and numerical (Jackson et al. 2004) solutions using poroviscosity theory have accurately simulated all three phases of consolidation shown in Fig. 7 using laboratory measurements of clays.

Suggested topic areas for future research

Additional research and development to improve the assessment, analysis and prediction of processes associated with the compaction of susceptible aquifer systems and the accompanying subsidence and ground ruptures are needed to support resource management and hazard mitigation measures. The suggested principal research topic areas include the hydromechanical behavior of aquitards, the role of horizontal deformation, the application of differential interferometry, and the regional-scale simulation of coupled groundwater flow and aquifer-system deformation.

Hydromechanical behavior of aquitards

In practical terms, aquitards, whether distinct hydrogeologic units (confining units) within an aquifer system or interbedded fine-grained deposits (interbeds) within an aquifer, principally are responsible for aquifer-system compaction and land subsidence accompanying the development of groundwater resources. The role of aquitards (especially thick ones) in this process is typified by the problems of determining flow in low permeability ($K<10^{-8}$ m/s) environments, thoroughly summarized by Neuzil (1986). The problems can be grouped roughly in terms of scale (temporal and spatial), measurement capability (laboratory and in situ) and coupling of stress-dependent processes. In practical terms, the problem of flow in low-permeability environments may be summarized as follows (Neuzil 1986): How can knowledge of behavior at small scales be extrapolated to large dimensions and long periods of time?

Scale

Presently, the practical temporal scale of interest in terms of historic and future (management planning horizons) land subsidence accompanying groundwater-resources development is on the order of a couple centuries—roughly, one in the past and one in the future. Thus, for purposes of this discussion the hydraulic (Darcian) and nonhydraulic (e.g. osmotic) flow processes that occur on geologic time scales (hundreds of centuries or more) are de-emphasized, realizing that the anthropogenic influences are superimposed on these natural processes. Generally, this includes the nonhydraulic flow processes, and those hydraulic flow processes related to continental tectonic and long-term cyclical climatic processes (e.g., glacial epochs). Osmotic flow is a nonhydraulic process that occurs on time scales similar to hydraulic flow, but osmotic flow only causes a change if the chemical driving forces (salinity patterns) change. In most of the settings of interest for subsidence that is not an issue.

Spatially, uncertainties related to small-scale hydraulic and material properties and behavior strongly affect the ability to understand and analyze large-scale behavior. This is a general problem related to heterogeneity and upscaling in hydrogeology (de Marsily et al. 2005; Gómez-Hernández 2006) associated with sampling, testing and measuring representative properties and responses both in the laboratory and in situ. For aquitards this general problem is compounded by low permeability, and

 DOI 10.1007/s10040-011-0775-5

some of the advantages of in situ vs. laboratory testing are diminished by difficulties both in imposing sufficient in situ hydraulic/mechanical stresses and in reliably measuring in situ responses in feasible time frames. Generally however, in normally- to over-consolidated alluvial and basin-fill sediments porosity (and thus groundwater storage) and permeability tend to decrease with increasing depth owing to processes of natural consolidation and diagenesis (Ingebritsen et al. 2006).

Measurement capability

In situ testing of aquitards was reviewed by Neuzil (1986) and includes single- (e.g. Bredehoeft and Papadopulos 1980) and multiple-well aquifer tests (e.g. Neuman and Witherspoon 1972), and large-scale consolidation tests (e.g. Riley 1969; see the previous section Extensometry). The former test is designed to directly stress and measure the transmissive properties of low permeability units but is limited by the volume of aquitard material that can be influenced by the test and the inadequacy of the method to provide reliable storage property estimates. Hydraulically, the latter two tests are more indirect and depend on the aquitard response (leakage) to stresses in the adjacent aquifers. These tests are capable of evaluating larger volumes of aquitard (generally, the affected aquitard volume is typified by large area and small thickness) but are limited by shortcomings in measuring capabilities of hydraulic heads in aquitards. Both of these tests frequently are used to estimate storage properties of the aquitards; the large-scale consolidation test is capable of directly measuring compaction of the aquifer system and estimating aquitard skeletal storage properties. Each of the in situ tests are limited by the number of available or emplaced wells and the population of discrete penetration depths used to characterize the process.

In the context of the aquitard drainage model, the previous maximum vertical effective stress of the aquitards typically is used to define a stress threshold beyond which the material deforms inelastically (visco-elastically) and within which deformation is elastic. Nearly all of the inelastic deformation generally is considered irreversible. The compressibility of the aquitards in the inelastic range of stress typically is 1–2 orders of magnitude larger than for the elastic range of stress (Riley 1998). Thus, depending on aquitard thickness, resulting compaction and accompanying subsidence is significantly larger for stresses greater than the preconsolidation stress. Historic, predevelopment groundwater levels, assuming fluid-pressure and thus effective-stress equilibrium, frequently are used to estimate steady-state heads and to constrain estimates of initial (immediately prior to groundwater resources development) preconsolidation stresses in the aquitards throughout the aquifer system. Typically, alluvial groundwater basins are overconsolidated; native preconsolidation stresses generally are somewhat larger than the predevelopment effective stresses, and land subsidence occurs only after substantial drawdowns have increased effective stresses beyond the native preconsolidation stress. Holzer (1981) identified various natural mechanisms that can result in an overconsolidated condition in alluvial basins; these mechanisms include removal of overburden by erosion, prehistoric groundwater-level declines, desiccation, and diagenesis. Because the preconsolidation stress is dependent on the total-stress history of the materials constituting the aquifer system, an accurate determination of the preconsolidation stress is not possible using predevelopment heads alone. Estimates can be constrained using other knowledge of the stress history of the system, for example geologic loading (depositional) and unloading (erosional), but this knowledge rarely is available in sufficient detail. Therefore, estimates of initial preconsolidation stresses constrained by historic groundwater levels often are highly uncertain. Nevertheless, when paired (temporally and spatially) groundwater-level and subsidence measurements are available this method has been used to estimate the initial preconsolidation stress (critical head) based on the groundwater level at which the rate of historical subsidence increased markedly (e.g., Holzer 1981; Anderson 1989; Sneed and Galloway 2000; Pavelko 2003). Laboratory consolidation tests could be used but they are rarely available for periods prior to the development of regional groundwater resources. However, in sufficiently thick confining units, where portions of the aquitards are not yet affected by head changes in the aquifers recent or contemporary laboratory consolidation tests on samples collected from those portions could be used. Transient (post-development) aquitard preconsolidation stresses can be determined from borehole extensometers using paired time series of groundwater level and compaction (Riley 1969). However, though useful, this method is problematic, especially for thick aquitards, because these water levels tend to be more representative of heads in the aquifers rather than the aquitards owing to hydrodynamic lag between aquifers and aquitards in the aquifer system. More often preconsolidation stress, constrained by in situ or laboratory data, is incorporated as a calibration parameter in numerical simulations of groundwater flow and aquifer-system compaction where the calibration parameters are computed (inverse problem) based in part on observed water levels and compaction and (or) subsidence (e.g., Hanson et al. 1990; Hanson and Benedict 1994; Galloway et al. 1998; Sneed and Galloway 2000; Leighton and Phillips 2003; Hanson et al. 2004; Liu and Helm 2008a, b). The simulated magnitude of subsidence is highly sensitive to predevelopment preconsolidation stress in many of the numerical models. The inverse problem is highly significant in low permeability environments because it may be the only means of estimating parameter values appropriate at large scale. The interactions between preconsolidation stress, elastic and viscoelastic strain, and flow are complex but important in a variety of settings. An

 DOI 10.1007/s10040-011-0775-5

important area for research now would seem to be investigation of methods to obtain reliable measurements of head and stress changes in thick aquitards accompanying groundwater resources development that can be used to formulate appropriate models of long-term aquifer-system compaction. The shortcomings of existing approaches and models are most pronounced for the prolonged flow transients in susceptible groundwater basins and limit the assessment of sustainable water-use strategies. This is relevant to the issue of ongoing head declines in thick aquitards and thereby compaction and subsidence even when heads in the aquifers stabilize or recover. This has been observed on seasonal and annual scales in a number of studies (e.g. Riley 1969; Wilson and Gorelick 1996; Pavelko 2000; Sneed and Galloway 2000; Hoffmann et al. 2003a), and the delayed flow transients have been addressed in the Dakota aquifer system where drawdowns have largely slowed or ceased but water is still presumably leaking from storage in the thick low-permeability shales (Konikow and Neuzil 2007).

Coupling of stress-dependent processes

More research and application is needed to address the stress dependence of aquitard storage and hydraulic conductivity. Though it is well known that these parameters decrease temporally with increasing effective stress and generally decrease with depth many regional groundwater-flow and aquifer-system compaction models do not simulate temporal- or depth-dependent variations in these parameters. Particular exceptions include Helm (1976), Neuman et al. (1982) and another using a 3D porous media model (Kim and Parizek 1999; Kim 2005; Kihm et al. 2007) where temporal variations in saturated hydraulic conductivity were included by making them dependent on the volume strain according to the relation

$$K = K_{\mathrm{o}}\left[\left(\frac{1}{n_{\mathrm{o}}}\right)(1+\varepsilon)^{2/3} - \left(\frac{1-n_{\mathrm{o}}}{n_{\mathrm{o}}}\right)(1+\varepsilon)^{-1/3}\right]^{3} \tag{18}$$

where K_{o} and n_{o} are the saturated hydraulic conductivity and effective porosity, respectively, prior to consolidation. No provision was made, however, for temporal changes in skeletal specific storage in this model. A generalized relation (Helm 1975) of the variation in skeletal specific storage with depth is shown in Fig. 8. The slopes of the secants AB and CB on Fig. 8 represent a linear approximation (Eq. 8) of $S_{s_{kv}}$ and $S_{s_{ke}}$, respectively. However, laboratory consolidation test data especially for fine-grained samples (clays and silts) indicate a strongly nonlinear stress-strain relation (e.g. solid lines on Fig. 8); empirically, the relation typically has been defined using the inverse slope of a best-fitting straight line to a plot of $log_{10}\sigma'_{zz}$ versus e. The slope, is a constant coefficient for the sample, the compression index, C_{c} or the recompression index, C_{r} for the inelastic and elastic ranges of stress, respectively, where for example:

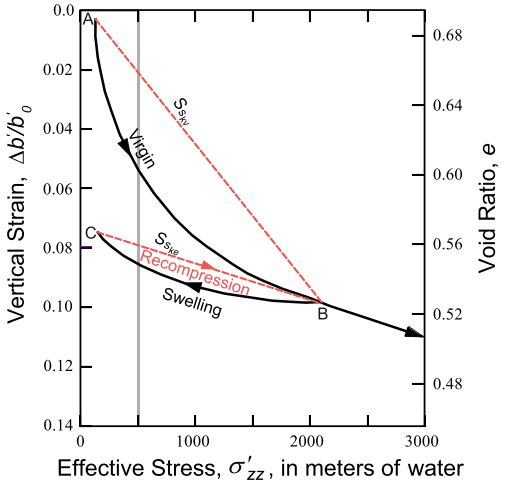

Fig. 8 Idealized stress-strain relation for a saturated volume element of compacting clay. The *black lines* indicate the empirical relation typically observed in laboratory consolidation tests and the *red lines* indicate the average slope of the strongly nonlinear portions of the empirical relation. These slopes for virgin compression and recompression represent average (constant) values of inelastic and elastic skeletal specific storage, respectively. The *grey line* indicates a maximum expected vertical effective stress in the depth interval of groundwater production for water-resources supplies. Modified from Helm (1975, Fig. 4)

$$C_{\mathrm{c}} = \frac{-\Delta e}{\Delta \log_{10}\sigma'_{zz}} \cong \frac{-de}{d(\log_{10}\sigma'_{zz})} \cong \frac{-\Delta e\sigma'_{zz}}{0.434\Delta\sigma'_{zz}}. \tag{19}$$

The relation between the compression and recompression indices and skeletal specific storage can be obtained by substituting Eq. 19 (and its equivalent for C_{r}) expressed in terms of $\Delta\sigma'_{zz}$ into Eq. 8 giving

$$Ss_{\mathrm{kv}} = \frac{0.434 C_{\mathrm{c}}\rho_{\mathrm{w}} g}{\sigma'(1+e_0)}, \tag{20}$$

and

$$Ss_{\mathrm{ke}} = \frac{0.434 C_{\mathrm{r}}\rho_{\mathrm{w}} g}{\sigma'(1+e_0)}. \tag{21}$$

Note that skeletal specific storage is inversely proportional to σ' in these formulations. Leake and Galloway (2007) argue, "For deep sediments, σ' will be large, and reductions in fluid pressure resulting from ground-water pumping are not likely to make large percentage changes in σ'. For that case Ss_{kv} and Ss_{ke} can be treated as constants with little resulting error. On the other hand, for shallow sediments where σ′ is relatively small, changes in fluid pressure could result in relatively large percentage changes in σ′." See Helm (1976), Jorgensen (1980) and Leake and Galloway (2007) for a summary of the development of Eqs. 19–21.

 DOI 10.1007/s10040-011-0775-5

The approach is generalized for regional 3D MODFLOW simulations in the SUB-WT Package (Leake and Galloway 2007) and demonstrated in a comparison of simulations using stress-independent and stress-dependent skeletal specific storage formulations for a groundwater basin in Antelope Valley, California (Leake and Galloway 2010). Compared to constant values of Ss_{kv} simulated in the existing calibrated model using IBS1 (Leighton and Phillips 2003), stress-dependent values of Ss_{kv} simulated using SUB-WT decline. For the upper unconfined aquifer (model layer 1) and the underlying middle confined aquifer (model layer 2), model computed values of Ss_{kv} at two locations (bench marks) decline during the simulation period (1915–1995) by 56 and 36%, respectively, for layer 1 and by 23 and 15%, respectively, for layer 2 (Fig. 9). Greater reductions occur in the shallow unconfined aquifer than in the underlying middle confined aquifer because the increase in σ' is greater in proportion to starting σ' of the upper unconfined aquifer. Despite the significant differences in Ss'_{kv} both models successfully simulated the historical time series of land subsidence at both bench marks, however, adjustments to starting values of Ss'_{kv} and differences in values assigned in model layers 1 (higher values) and 2 (lower values) were necessary for the depth-dependent (SUB-WT) simulations. These results underscore the nonuniqueness of the problem and the critical need for further development of more accurate and powerful regional modeling tools such as poroviscosity theory, despite its greatly increased data requirements. It could be argued that the appropriate governing properties can only be determined in situ—at the length and time scales of interest—but that in situ methods yield nonunique results as described here.

The limitations of using stress-independent skeletal specific storage formulations in settings where transient compaction is occurring include: (1) overestimation of subsidence projections under conditions of increasing σ' owing to unaccounted future reductions in skeletal specific storage; (2) the tendency to misrepresent compaction and head distributions in regional unconfined aquifers that undergo large drawdowns; (3) the possibility of misrepresenting the vertical distribution of compaction by specifying identical bulk values of skeletal specific storage for multiple model layers with interbedded aquitards, which tacitly assumes that deeper layers are lithologically different such that they are more compressible than shallower layers—a condition that may exist but typically does not. In a 1D vertical simulation of a 4.69-m thick homogeneous, doubly-draining aquitard from Pixley, California, Helm (1976); Fig. 10) concluded that K'_z is proportionally more reduced than Ss'_{kv} and suggests that simulating thick aquitards with stress-independent hydraulic parameters (e.g. using the SUB Package) can lead not only to overestimation of ultimate compaction but also to underestimation of τ' (Eq. 11).

These inaccuracies must be weighed against inaccurate characterizations of the aquifer system at a more fundamental level. For example, identification and definition of the aquitards and their hydromechanical properties, and the uncertainties regarding gradational characteristics of aquitard boundaries, and the heterogeneity of aquitards and aquifers are all important in a site-specific, predictive context. For regional-scale models this level of detail likely is not feasible and as such only generic behaviors may be simulated.

Additionally, further challenges of accurately simulating the behavior of compacting aquitards can occur when the poromechanical and physical properties of the media are significantly altered such that the flow conditions through the material can be greatly modified. Such is the case with the fluvio-lacustrine sediments occupying the Mexico basin surrounding Mexico City where in parts of the basin subsidence rates have exceeded 400 mm/yr and remained at an astonishingly high level for decades, and more than 13.5 m of subsidence has accrued (Auvinet 2009). Rates of nearly 350 mm/yr have been measured recently (Cabral-Cano et al. 2008). The large subsidence is attributed not only to large pumping rates but also to the

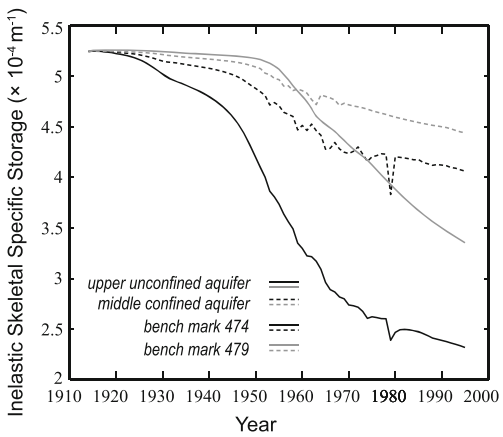

Fig. 9 Simulated temporal variations in inelastic skeletal specific storage for two model layers representing an upper unconfined aquifer and an underlying middle confined aquifer at locations of bench marks *474* and *479* in Antelope Valley, California. Modified from Leake and Galloway (2010)

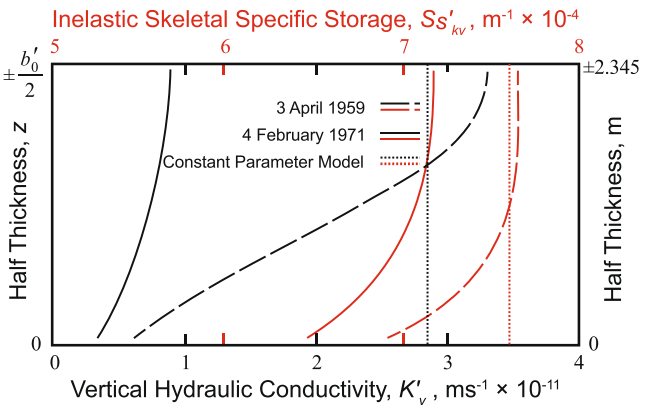

Fig. 10 Temporal (1959–1971) and spatial (depth) distributions of inelastic skeletal specific storage (*red curves*) and vertical hydraulic conductivity (*black curves*) simulated in a thick (4.69 m) doubly draining aquitard from Pixley, California. Simulated values are shown only for the half thickness of the aquitard owing to vertical symmetry with respect to the aquitard horizontal midplane $\left(z = \pm\frac{b'_0}{2} = 2.345m\right)$. Modified from Helm (1976; Fig. 13))

DOI 10.1007/s10040-011-0775-5

nature of the compacting clayey materials, which are described as allophanes. Allophanes are unique in that intermolecular water became part of the structure of the material during deposition and diagenesis (Carreón-Freyre 2010). Prior to consolidation these allophanes can possess gravimetric water contents in excess of 400% by volume (Alberto-Jaime and Méndez-Sánchez 2010). Once these clays have been stressed and the water has been removed they can shrink to 25–30% of their original volume. Furthermore, these allophanes experience virtually no swelling upon rewetting (Alberto-Jaime and Méndez-Sánchez 2010; D. Carreón-Freyre, Centro de Geociencias UNAM, personal communication, 2010). Upon compaction, the flow properties of these materials are greatly altered. Typical clays result in a reduction in overall vertical hydraulic diffusivity $\left(K_z'/Ss'\right)$ as a result of a loss of water content. These deposits, however, may conversely experience an increase in vertical hydraulic diffusivity because of their greatly reduced thickness, changed morphology and poromechanical behavior. Ortega-Guerrero et al. (1999) developed a 1D subsidence model of the Chalco Basin region of Mexico City. Using log-dependent changes in void ratio and hydraulic conductivity as a function of stress, they aimed to replicate existing subsidence patterns at a single point in the Chalco Basin. They deftly adapted thickness changes of model node locations to more adequately simulate the transient spatial location of compacting units and were able to reproduce quite well the observed compaction record at their site. Their model, however, attempted only to quantify primary compaction and was not flow-dependent, which would create a tremendous challenge for multi-dimensional poroelasticity regional flow models.

Poroviscosity theory, on the other hand, would likely be capable of replicating not only the material property changes of the aquitards, but also the flow property changes through them. The key in poroviscosity theory would be to adequately describe the poroviscous constant A (Eq. 15), using laboratory experiments. The future challenge will be to expand 3D poroviscosity theory (Jeng 2005) to an applicable regional-scale model with identifiable boundary conditions so that it could be applied to settings such as the Mexico City basin. For one dimension, Jackson et al. (2004) have shown the viability of the poroviscous model. However, Jeng (2005) concluded that adapting the poroviscous theory to multiple dimensions in numerical models would be a tremendous challenge unless certain limitations and assumptions for boundary conditions at the regional scale are made. This represents an important direction for subsidence research.

Horizontal motion

Horizontal displacement occurs in aquifer systems in response to pumping and seasonal recharge/discharge stresses (Wolff 1970; Carpenter 1993; Helm 1994; Hsieh 1996; Bawden et al. 2001; Burbey 2001a, b; Li 2007a, b, c). However, in areas of subsidence attributed to fluid withdrawal, horizontal displacement of the land surface has been measured only at a few places. Fewer examples exist where these measurements have been incorporated into analyses and simulations of aquifer-system deformation, but when observed horizontal displacements have been used to constrain numerical models they have been shown to reflect the hydraulic properties of the aquifer system and were therefore used to characterize the aquifer system in ways that hydraulic heads alone could not (Burbey 2006; Burbey et al. 2006). In compacting aquifer systems, the subsidence generally is regional and widespread so that regional-scale lateral (sub-horizontal) strains are rarely as large as 2 ppm and resulting regional-scale tilts generally are less than about 1.16×10^{-3} radians (240 arcseconds). Locally, however, lateral strains may be large such as near pumping wells where hydraulic gradients are large, near where the aquifer system thins abruptly above inflections in the basement topography of the aquifer system, and near the boundaries of hydrogeologic units with contrasting hydraulic and (or) mechanical properties (Galloway et al. 2008). More research is needed to elucidate the role of horizontal strains in the formation of earth fissures in basins susceptible to aquifer-system compaction. Recent investigations reveal the importance not only of horizontal strain in the development of some earth fissures, but also of shear on vertical planes and rotational stresses (Budhu 2011). Lithologic variations such as the degree of cementation in alluvium (Budhu 2011) and geologic structures such as faults play an important role not only in the development of fissures but also in their location (Hernandez-Marin and Burbey 2009, 2010a).

Differential interferometry

Synthetic aperture radar (SAR)

Galloway and Hoffmann (2007) noted that new and future InSAR capabilities would enhance understanding of the coupled hydromechanical responses of complex aquifer systems to natural and anthropogenic stresses. The successful implementations of the ALOS-PALSAR (2006–present), COSMO-SkyMed constellation (2007–present), TerraSAR-X (2007–present) and TanDEM-X (2010–present) SAR satellite platforms are helping. InSAR derived displacement data used in concert with other hydrogeologic information can be used to improve definition of the structural, depositional, and hydromechanical heterogeneity of thick alluvial aquifer systems, to delineate areas prone to earth fissures and residual compaction, to identify elastic and inelastic strain regimes, to define preconsolidation thresholds, and to provide estimates of some of the governing aquifer-system hydraulic properties (e.g. Ss'_{kv} and $K_{z'}$ in Eq. 9). Specific applications development is needed not only to improve integration of ground-based geodetic data with InSAR, but also to improve the use of InSAR in constraining hydrogeologic models, and thereby improve resource assess-

 DOI 10.1007/s10040-011-0775-5

ments and potentially, sustainable development of these systems susceptible to aquifer-system compaction. This kind of integration of assessment information has been used to provide improved mapping, monitoring, and insights into the controlling geologic, hydrologic, and anthropogenic factors (e.g. Phillips et al. 2003; Teatini et al. 2005), but generally is underutilized by hydrogeologists (Hoffmann 2005). Increasing use of numerical groundwater flow models to evaluate optimal alternative management strategies that include subsidence mitigation is needed (e.g. Danskin et al. 2003; Phillips et al. 2003; Danskin et al. 2006). As Hoffmann et al. (2003a) have shown, InSAR can be used to constrain and improve these models, but because time constants of compacting aquifer systems typically can be decades or longer, the ability to constrain these systems using SAR data available only since 1992 has been limited. As more SAR data suitable for interferometry become available, better models, predictions and management can result. Other promising future applications of InSAR include evaluating horizontal deformation in aquifer systems (e.g. Burbey 2001a,b, 2002, 2005; Hoffmann and Zebker 2003; Dehghani et al. 2010; Lubis et al. 2011), and using small baseline subset (SBAS) techniques (Berardino et al. 2002) for improving conventional InSAR mapping over agricultural areas (Reeves et al. 2010).

PSI can contribute to each of the applications discussed in the previous and should enhance capabilities to detect and monitor ground displacements in critical agricultural areas heavily dependent on groundwater supplies and other areas where coherent InSAR is limited by poor temporal coherence. PSI has been more widely applied in Europe and many potential applications exist in North America, Asia and elsewhere. The use of PSI to monitor aquifer-system compaction and subsidence along the California Aqueduct in the agricultural San Joaquin Valley, California is currently underway (M. Sneed, US Geological Survey, personal communication, 2011). A hybrid approach using PSI and conventional InSAR shows promise for monitoring subsidence in some agricultural areas (e.g. Dehghani et al. 2010).

Synthetic aperture sonar (SAS)

Developments in SAS interferometry for underwater, buried mine detection, marine archeological exploration, bathymetric mapping and change detection of the seabed (Sæbø 2010) hold promise for monitoring sea floor subsidence. Most of the potential applications would be applicable to subsidence induced by the extraction of oil and gas from near shore and offshore hydrocarbon reservoirs. New techniques using autonomous underwater vehicles (AUVs) overcome some of the problems associated with sonic-wave multipath propagation errors associated with salinity and temperature variations, and platform motion errors associated with variable environmental conditions at the sea surface. Research on the deployment of arrays of stable artificial sonic targets on the seafloor shows promise in mitigating the temporal decorrelation problems associated with dynamic sediment transport on the seabed (S. Biagini, NURC–Italy, unpublished paper, 2010; De Paulis et al. 2010).

Simulation

Future developments are needed in the general approaches to simulating subsidence accompanying aquifer-system deformation induced by groundwater extraction—the aquitard drainage model and poroelasticity/poroviscosity models. The aquitard drainage model approach embodied in the MODFLOW simulation capabilities has proven useful for regional simulations of groundwater flow, aquifer-system compaction and land subsidence. Its strength is the ability to incorporate a wide variety of hydrogeologic features along with generally simple subsidence formulations expressed in hydrogeologic terms in a single modeling system. As such it has been used in groundwater systems where subsidence mitigation is a component of the management of water resources. Its principal weakness derives from its use of the 1D storage coefficient (assumption of vertical stress and strain only) which renders the coupling of fluid-pressure (volume stress) changes with deformation (uniaxial-vertical) incapable of simulating horizontal components of displacement; therefore, this approach is not applicable in regions where horizontal motions are significant—particularly at local scales as previously discussed. Another shortcoming is the inability presently to model aquifer systems that simultaneously exhibit features simulated by the SUB Package (time-dependent drainage and compaction of thick aquitards) and the SUB-WT Package (changing geostatic stress and stress-dependent skeletal specific storage). Incorporation of these capabilities into a single subsidence simulator would enhance flexibility and facilitate applications to commonly encountered developed systems with a water-table aquifer overlying a confined aquifer system.

The poroelasticity and poroviscosity modeling approaches more rigorously describe the coupled processes of groundwater flow and the 3D deformation of aquifer systems. Applications of these approaches to aquifer systems susceptible to groundwater-extraction-induced subsidence largely have focused on exploring and explaining possible behaviors of deforming aquifer systems where horizontal motion is expected. The paucity of three-component deformation data at depth and at land surface has been one factor limiting their wider use. Other significant factors limiting their use include the more complex formulation of the methods, their intensive computational requirements to simulate realistic flow and aquifer-system deformation problems at regional scales, and the scarcity of publicly accessible modeling software and the data on aquifer-system properties sufficient to constrain these models. For example, the applications of the poroelastic model previously presented by Kim (2005) and Kihm et al. (2007) were for small aquifer systems, generally less than 1,000 m×1,000 m×50-m thick. Both studies indicated the need for more 3D head and

 DOI 10.1007/s10040-011-0775-5

deformation data to constrain the models. Recent applications of these approaches have been effective in providing insights into the accumulation of groundwater-extraction induced stresses and strains near earth fissures and pre-existing surface faults, and into the genesis of earth fissures (Hernandez-Marin and Burbey 2009, 2010a, b). Future developments will benefit from applications where simulations can be constrained by enhanced three-component displacement data obtained in deforming aquifer systems.

Acknowledgements This work was encouraged by Shemin Ge (Editor, *Hydrogeology Journal*) and supported by the USGS Cooperative Water and Groundwater Resources Programs, and the National (US) Science Foundation. The UNESCO Working Group on Land Subsidence and the American Society of Civil Engineers' Managed Aquifer Recharge Committee, Subcommitte on Land Subsidence provided early reviews of portions of the manuscript. Peer reviews by Stanley A. Leake, Zhong Lu, Chris E. Neuzil (all USGS), two anonymous reviewers and David F. Boutt (Associate Editor, *Hydrogeology Journal*) greatly improved the manuscript. This review inevitably omits many significant contributions to subsidence research. Errors of omission and commission are the sole responsibility of the authors.

References

Abidin HZ, Andreas H, Gumilar I, Gamal M, Fukuda Y, Deguchi T (2009) Land subsidence and urban development in Jakarta (Indonesia). 7th FIG Regional Conference Spatial Data Serving People: Land Governance and the Environment: Building the Capacity, Hanoi, Vietnam, 19–22 October 2009. http://www.fig.net/vietnam/. Cited 31 May 2011

ADWR (2011) Maps of land subsidence areas in Arizona: Scottsdale subsidence feature. ADWR, Phoenix, AZ. http://www.adwr.state.az.us/azdwr/Hydrology/Geophysics/documents/ScottsdaleArea2004to2010_8x11.pdf. Cited 31 May 2011

Alberto-Jaime P, Méndez-Sánchez E (2010) Evolution of Mexico City clay properties affected by land subsidence. In: Carreón-Freyre D, Cerca M, Galloway DL, Silva-Corona JJ (eds) Land subsidence, associated hazards and the role of natural resources development (EISOLS 2010). IAHS Publ. 339, IAHS, Wallingford, UK, pp 232–234

Amelung F, Galloway DL, Bell JW, Zebker HA, Laczniak RL (1999) Sensing the ups and downs of Las Vegas: InSAR reveals structural control of land subsidence and aquifer-system deformation. Geology 27(6):483–486

American Society of Photogrammetry and Remote Sensing (2004) ASPRS guidelines: vertical accuracy reporting for LiDAR data,ver 1.0. American Society of Photogrammetry and Remote Sensing Lidar Committee. http://www.asprs.org/a/society/committees/standards/Vertical_Accuracy_Reporting_for_Lidar_Data.pdf. Cited 13 July 2011

Anderson SR (1989) Potential for aquifer compaction, land subsidence, and earth fissures in Avra Valley, Pima and Pinal Counties, Arizona. USGS Hydrologic Investigations Atlas 718, 3 sheets, scale 1:250000. http://pubs.er.usgs.gov/usgspubs/ha/ha718. Cited 22 Jan 2011

Anderssohn J, Wetzel HU, Walter T, Motagh M (2008) Measurement of land subsidence in the Kashmar Valley, northeast Iran, using satellite radar interferometry. ESA SP 649, European Space Agency, Paris

Auvinet G (2009) Land subsidence in Mexico City. In: Auvinet GY, Juárez M (eds) Geotechnical engineering in urban areas affected by land subsidence. Volume prepared by ISSMGE Technical Committee 36 for XVII ISSMGE Conference, Alexandria, Egypt, 2009. Mexican Society of Soil Mechanics, Mexico City, pp 3–11

Barends FBJ, Brouwer FJJ, Schröder FH (eds) (1995) Land subsidence. Proceedings of the Fifth International Symposium on Land Subsidence, The Hague, Netherlands, Oct 1995. IAHS Publ. 234, IASH, Wallingford, UK. http://iahs.info/redbooks/234.htm. Cited 13 July 2011

Barrientos B, Cerca M, García-Márquez J, Hernández-Bernal C (2008) Three-dimensional displacement fields measured in a deforming granular-media surface by combined fringe projection and speckle photography. J Opt A: Pure Appl Opt 10. doi:10.1088/1464-4258/10/10/104027

Bawden GW (2002) Optimizing GPS arrays to image both tectonic and anthropogenic deformation. EOS Trans 83:52, abstract G22A-11

Bawden GW, Thatcher W, Stein RS, Hudnut KW, Peltzer G (2001) Tectonic contraction across Los Angeles after removal of groundwater pumping effects. Nature 412:812–815

Beaver J, Tatlow M, Cohen D, Marra M (2005) Monitoring subsidence trends in Phoenix with SAR interferometry. EOS Trans 86:52, abstract G51C-0852

Bell JW, Amelung F, Ramelli A, Blewitt G (2002) Land subsidence in Las Vegas, Nevada, 1935–2000: new geodetic data show evolution, revised spatial patterns, and reduced rates. Env Eng Geosci 8(3):155–174

Bell JW, Amelung F, Ferretti A et al (2008) Permanent scatterer InSAR reveals seasonal and long-term aquifer system response to groundwater pumping and artificial recharge. Water Resour Res 44:W02407. doi:10.1029/2007WR006152

Berardino P, Fornaro G, Lanari R, Sansosti E (2002) A new algorithm for surface deformation monitoring based on small baseline differential SAR interferograms. ITGRS 40(11):2375–2383

Biot MA (1941) General theory of three-dimensional consolidation. J App Phys 12:155–164

Bonsignore F, Bitelli G, Chahoud A, Macini P, Mesini E, Severi P, Villani B, Vittuari L (2010) Recent extensometric data for the monitoring of subsidence in Bologna (Italy). In: Carreón-Freyre D, Cerca M, Galloway DL, Silva-Corona JJ (eds) Land subsidence, associated hazards and the role of natural resources development (EISOLS 2010). IAHS Publ. 339, IAHS, Wallingford, UK, pp 333–338

Borchers JW (ed) (1998) Land subsidence case studies and current research. Proceedings of the Dr. Joseph F. Poland Symposium on Land Subsidence, 4–5 Oct 1995, Sacramento, California. Spec. Publ. 8, Assoc. Eng. Geol., Denver CO, Star, Belmont, CA

Bredehoeft JD, Papadopulos SS (1980) A method for determining the hydraulic properties of tight formations. Water Resour Res 16(1):233–238

Buckley SM, Rosen PA, Hensley S, Tapley BD (2003) Land subsidence in Houston, Texas, measured by radar interferometry and constrained by extensometers. J Geophys Res 108 (B11):2542. doi:10.1029/2002JB001848, Cited 31 May 2011

Budhu M (2011) Earth fissure formation from the mechanics of groundwater pumping. Int J Geomech 11(1). doi:10.1061/(ASCE)GM.1943-5622.0000060

Burbey TJ (2001a) Stress-strain analyses for aquifer-system characterization. Ground Water 39(1):128–136

Burbey TJ (2001b) Storage coefficient revisited: Is purely vertical strain a good approximation? Ground Water 39(3):458–464

Burbey TJ (2002) The influence of faults in basin-fill deposits on land subsidence, Las Vegas, Nevada, USA. Hydrogeol J 10 (5):525–538

Burbey TJ (2005) Use of vertical and horizontal deformation data with inverse models to quantify parameters during aquifer testing. In: Zhang A, Gong S, Carbognin L, Johnson AI (eds) Land subsidence. Proceedings of the 7th International Symposium on Land Subsidence, Oct 2005, vol 2. Shanghai Scientific, Shanghai, PRC, pp 560–569

Burbey TJ (2006) Three-dimensional deformation and strain induced by municipal pumping, part 2: numerical analysis. J Hydrol 330(3–4):422–434

Burbey TJ, Helm DC (1999) Modeling three-dimensional deformation in response to pumping of unconsolidated aquifers. Env Eng Geosci 5:199–212

Burbey TJ, Warner SM, Blewitt G, Bell JW, Hill E (2006) Three-dimensional deformation and strain induced by municipal pumping, part 1: analysis of field data. J Hydrol 319(1–4):123–142

Cabral-Cano E, Dixon TH, Miralles-Wilhelm F, Díaz-Molina O, Sánchez-Zamora O, Carande RE (2008) Space geodetic imaging of rapid ground subsidence in Mexico City. GSA Bull 120(11–12):1556–1566

Calderhead AI, Martel R, Alasset PJ, Rivera A, Garfias J (2010) Land subsidence induced by groundwater pumping, monitored by D-InSAR and field data in the Toluca Valley, Mexico. Can J Remote Sens 36(1):9–23

Calderhead AI, Therrien R, Rivera A, Martel R, Garfias J (2011) Simulating pumping-induced regional land subsidence with the use of InSAR and field data in the Toluca Valley, Mexico. Adv Water Resour 34:83–97. doi:10.1016/j.advwatres.2010.09.017

Canuti P, Casagli N, Farina P, Marks F, Ferretti A, Menduni G (2005) Land subsidence in the Arno River Basin studied through SAR interferometry. In: Zhang A, Gong S, Carbognin L, Johnson AI (eds) Land subsidence. Proceedings of the Seventh International Symposium on Land Subsidence, vol 1. Shanghai Scientific, Shanghai, pp 407–416

Carbognin L, Gambolati G, Johnson AI (eds) (2000) Land subsidence. Proceedings of the Sixth International Symposium on Land Subsidence, Ravenna, Italy, 24–29 Sept 2000, vols 1–2. La Garagola, Padova, Italy,

Carpenter MC (1993) Earth-fissure movements associated with fluctuations in ground-water levels near the Picacho Mountains, south-central Arizona, 1980–84. US Geol Surv Prof Pap 497-H. http://pubs.er.usgs.gov/usgspubs/pp/pp497H. Cited 13 July 2011

Carreón-Freyre D (2010) Land subsidence processes and associated ground fracturing in central Mexico. In: Carreón-Freyre D, Cerca M, Galloway DL, Silva-Corona JJ (eds) Land subsidence, associated hazards and the role of natural resources development (EISOLS 2010). IAHS Publ. 339, IAHS, Wallingford, UK, pp 149–157

Carreón-Freyre, D, Cerca, M, Galloway DL, Silva-Corona JJ (eds) (2010) Land subsidence, associated hazards and the role of natural resources development (EISOLS 2010). IAHS Publ. 339, IAHS, Wallingford, UK

Carruth RL, Pool DR, Anderson CE (2007) Land subsidence and aquifer-system compaction in the Tucson Active Management Area, south-central Arizona, 1987–2005. US Geol Surv Sci Invest Rep 2007–5190. http://pubs.usgs.gov/sir/2007/5190/. Cited 13 July 2011

Chatterjee RS, Fruneau B, Rudant JP, Roy PS, Frison PL, Lakhera RC, Dadhwal VK, Saha R (2006) Subsidence of Kolkata (Calcutta) City, India during the 1990s as observed from space by Differential Synthetic Aperture Radar Interferometry (D-InSAR) technique. Remote Sens Environ 102(1–2):176–185

Cooper HH Jr (1966) The equation of groundwater flow in fixed and deforming coordinates. J Geophys Res 71:4785–4790

Danskin WR, Kasmarek MC, Strom EW (2003) Optimal withdrawal of elastically stored ground water in the Chicot Aquifer, Houston area, Texas. In: Prince KR, Galloway DL (eds) US Geological Survey Subsidence Interest Group Conference, Proceedings of the technical meeting, Galveston, Texas, 27–29 November 2000, US Geol Surv Open-File Rep 03–308, pp 39–48. http://pubs.usgs.gov/of/2003/ofr03-308/pdf/OFR03-308.pdf. Cited 13 July 2011

Danskin WR, McPherson KR, Woolfenden LR (2006) Hydrology, description of computer models, and evaluation of selected water-management alternatives in the San Bernardino area, California. US Geol Surv Open-File Rep 2005–1278. http://pubs.usgs.gov/of/2005/1278/. Cited 13 July 2011

de Marsily Gh, Delay F, Gonçalvès J et al (2005) Dealing with spatial heterogeneity. Hydrogeol J 13:161–183

De Paulis R, Prati C, Scirpoli S, Sletner PA, Tesei A (2010) Measuring seabed altimetric variations with a repeat-track SAS interferometry experiment: processing and results. In: Carreón-Freyre D, Cerca M, Galloway DL, Silva-Corona JJ (eds) Land subsidence, associated hazards and the role of natural resources development (EISOLS 2010). IAHS Publ. 339, IAHS, Wallingford, UK, pp 358–363

Dehghani M, Hooper A, Hanssen RF, Zoej MJV, Saatchi S, Entezam I (2010) Hybrid conventional and persistent scatterer SAR interferometry for land subsidence monitoring in Tehran Basin, Iran. Proceedings FRINGE Workshop 2009, Frascati, Italy, 30 Nov–4 Dec 2009

Densmore J, Ellett K, Howle J, Carpenter, M, Sneed M (2010) Measuring land-surface deformation on Bicycle Lake playa, Fort Irwin, California, USA. In: Carreón-Freyre D, Cerca M, Galloway DL, Silva-Corona JJ (eds) Land subsidence, associated hazards and the role of natural resources development (EISOLS 2010). IAHS Publ. 339, IAHS, Wallingford, UK, pp 39–43

Don NC, Hang NTM, Araki H, Yamanishi H, Koga K (2006) Groundwater resources management under environmental constraints in Shiroishi of Saga plain, Japan. Environ Geol 49:601–609. doi:10.1007/s00254-005-0109-9

Epstein VJ (1987) Hydrologic and geologic factors affecting land subsidence near Eloy, Arizona. US Geol Surv Water Resour Invest Rep 87–4143. http://pubs.er.usgs.gov/usgspubs/wri/wri874143. Cited 13 July 2011

Faunt CC (ed) (2009) Ground-water availability of California's Central Valley Aquifer, California. US Geol Surv Prof Pap 1766. http://pubs.usgs.gov/pp/1766/. Cited 13 July 2011

Federal Geodetic Control Committee (1984) Standards and specifications for geodetic control networks. National Geodetic Survey, NOAA, Rockville, MD. http://www.ngs.noaa.gov/FGCS/tech_pub/1984-stds-specs-geodetic-control-networks.htm. Cited 13 July 2011

Ferretti A, Prati C, Rocca F (2000) Nonlinear subsidence rate estimation using permanent scatterers in differential SAR interferometry. IEEE Trans Geosci Remote Sens 38(5):2202–2212

Ferretti A, Prati C, Rocca F (2001) Permanent scatterers in SAR interferometry. IEEE Trans Geosci Remote Sens 39(1):8–20

Ferretti A, Novali R, Bürgmann R, Hilley G, Prati C (2004) InSAR permanent scatterer analysis reveals ups and downs in the San Francisco Bay Area. Eos 85(34):317–324

Floyd RP (1978) Geodetic bench marks. National Oceanic and Atmospheric Administration Manual NOS NGS 1. http://www.ngs.noaa.gov/PUBS_LIB/GeodeticBMs.pdf. Cited 13 July 2011

Fruneau B, Sarti F (2000) Detection of ground subsidence in the city of Paris using radar interferometry: isolation of deformation from atmospheric artifacts using correlation. Geophys Res Lett 27(24):3981–3984. doi:10.1029/2000GL008489

Gabriel AK, Goldstein RM, Zebker HA (1989) Mapping small elevation changes over large areas: differential radar interferometry. J Geophys Res 94:9183–9191

Galloway DL, Hoffmann J (2007) The application of satellite differential SAR interferometry-derived ground displacements in hydrogeology. Hydrogeol J 15(1):133–154. doi:10.1007/s10040-006-0121-5

Galloway DL, Hudnut KW, Ingebritsen SE, Phillips SP, Peltzer G, Rogez F, Rosen PA (1998) Detection of aquifer system compaction and land subsidence using interferometric synthetic aperture radar, Antelope Valley, Mojave Desert, California. Water Resour Res 34(10):2573–2585

Galloway D, Jones DR, Ingebritsen SE (eds) (1999) Land subsidence in the United States. US Geol Surv Circ 1182. http://pubs.usgs.gov/circ/circ1182/. Cited 13 July 2011

Galloway DL, Bawden GW, Leake SA, Honegger DG (2008) Land subsidence hazards. In: Baum RL et al (eds) Landslide and land subsidence hazards to pipelines. US Geol Surv Open-File Rep 2008–1164, chap. 2. http://pubs.usgs.gov/of/2008/1164/. Cited 13 July 2011

Gambolati G, Freeze RA (1973) Mathematical simulation of the subsidence of Venice, 1: theory. Water Resour Res 9(3):721–733

Gambolati G, Teatini P, Baú D, Ferronato M (2000) Importance of poro-elastic coupling in dynamically active aquifers of the Po River basin, Italy. Water Resour Res 36(9):2443–2459

Gambolati G, Teatini P, Ferronato M (2005) Anthropogenic land subsidence. In: Anderson MG (ed) Encyclopedia of hydrological sciences. Wiley, Wiley Online Library, 17 pp. http://

onlinelibrary.wiley.com/book/10.1002/0470848944;jsessionid=5ECA1E367646E2E75793ACE0CFBFDF11.d02t02. Cited 29 July 2011
Gómez-Hernández JJ (2006) Complexity. Ground Water 44(6):782–785
Guarnieri AM, Rocca F (1999) Combination of low- and high-resolution SAR images for differential interferometry. IEEE Trans Geosci Rem Sens 37:2035–2049
Hanson RT (1989) Aquifer-system compaction, Tucson Basin and Avra Valley, Arizona. US Geol Surv Water Resour Invest Rep 88–4172. http://pubs.er.usgs.gov/usgspubs/wri/wri884172. Cited 13 July 2011
Hanson RT, Benedict JF (1994) Simulation of ground-water flow and potential land subsidence, upper Santa Cruz Basin, Arizona. US Geol Surv Water Resour Invest Rep 93–4196. http://pubs.er.usgs.gov/usgspubs/wri/wri934196. Cited 13 July 2011
Hanson RT, Anderson SR, Pool DR (1990) Simulation of ground-water flow and potential land subsidence, Avra Valley, Arizona. US Geol Surv Water Resour Invest Rep 90–4178. http://pubs.er.usgs.gov/usgspubs/wri/wri904178. Cited 13 July 2011
Hanson RT, Li Z, Faunt C (2003a) Application of the multi-node well package to the simulation of regional-aquifer systems in the Santa Clara Valley, California: MODFLOW and More 2003: Understanding through Modeling. Conference proceedings. International Ground Water Modeling Center, Golden, CO, 16–19 September 2003, pp 74–78
Hanson RT, Martin P, Koczot KM (2003b) Simulation of ground-water/surface-water flow in the Santa Clara-Calleguas ground-water basin, Ventura County, California. US Geol Surv Water Resour Invest Rep 02–4136. http://pubs.usgs.gov/wri/wri024136/text.html. Cited 13 July 2011
Hanson RT, Li Z, Faunt C (2004) Documentation of the Santa Clara Valley regional ground-water/surface-water flow model, Santa Clara Valley, California. US Geol Surv Sci Invest Rep 2004–5231. http://pubs.usgs.gov/sir/2004/5231/. Cited 13 July 2011
Harbaugh AW (2005) MODFLOW-2005, The U.S. Geological Survey modular ground-water model: the ground-water flow process. US Geol Surv Tech Methods 6-A16. http://pubs.usgs.gov/tm/2005/tm6A16/. Cited 13 July 2011
Harbaugh AW, Banta ER, Hill MC, McDonald MG (2000) MODFLOW-2000, the U.S. Geological Survey modular ground-water model: user guide to modularization concepts and the ground-water flow process. US Geol Surv Open-File Rep 2000–92. http://water.usgs.gov/nrp/gwsoftware/modflow2000/ofr00-92.pdf. Cited 13 July 2011
Hayashia T, Tokunaga T, Aichi M, Shimada J, Taniguchi M (2009) Effects of human activities and urbanization on groundwater environments: an example from the aquifer system of Tokyo and the surrounding area. Sci Total Environ 407:3165–3172. doi:10.1016/j.scitotenv.2008.07.012
Helm DC (1972) Simulation of aquitard compaction due to changes in stress. Trans Am Geophys Union 53(11):979, abstracts
Helm DC (1975) One-dimensional simulation of aquifer system compaction near Pixley, Calif. 1: constant parameters. Water Resour Res 11(3):465–478
Helm DC (1976) One-dimensional simulation of aquifer system compaction near Pixley, Calif. 2: stress-dependent parameters. Water Resour Res 1(3):375–391
Helm DC (1978) Field verification of a one-dimensional mathematical model for transient compaction and expansion of a confined aquifer system, Verification of mathematical and physical models in hydraulic engineering. Proc 26th Hydraul Div Specialty Conf., College Park, MD. Amer. Soc. Civil Eng., Washington, DC, pp 189–196
Helm DC (1984a) Field-based computational techniques for predicting subsidence due to fluid withdrawal. In: Holzer TL (ed) Man-induced land subsidence. Rev Eng Geol 6:1–22
Helm DC (1984b) Latrobe Valley subsidence predictions: the modeling of time-dependent ground movement due to ground-water withdrawal. Joint Report of Fuel Department and Design Engineering and Environment Department, State Electricity Commission of Victoria, Melbourne
Helm DC (1986) COMPAC: a field-tested model to simulate and predict subsidence due to fluid withdrawal. Austral Geomechan Comput Newslett 10:18–20
Helm DC (1987) Three-dimensional consolidation theory in terms of the velocity of solids. Geotechnique 37(3):369–392
Helm DC (1994) Horizontal aquifer movement in a Theis-Thiem confined aquifer system. Water Resour Res 30(4):953–964
Helm DC (1998) Poroviscosity. In: Borchers JW (ed) Land subsidence case studies and current research. Proceedings of the Dr. Joseph F. Poland Symposium on Land Subsidence, vol 8, 4–5 Oct 1995, Sacramento, CA. Spec. Publ., Assoc. Eng. Geol., Star, Belmont, CA, pp 395–405
Hernandez-Marin M, Burbey TJ (2009) The role of faulting on surface deformation patterns from pumping induced ground-water flow. Hydrogeol J 17(8):1859–1875. doi:10.1007/s10040-009-0501-8
Hernandez-Marin M, Burbey TJ (2010a) Controls on initiation and propagation of pumping-induced earth fissures: insights from numerical simulations. Hydrogeol J 18(8):1773–1785. doi:10.1007/s10040-010-0642-9
Hernandez-Marin M, Burbey TJ (2010b) On the mechanisms for earth fissuring in Las Vegas valley: a numerical analysis of pumping-induced deformation and stress. In: Carreón-Freyre D, Cerca M, Galloway DL (eds) Land subsidence, associated hazards and the role of natural resources development. Proceedings of the Eighth Int. Symp. on Land Subsidence, Santiago de Querétaro, Mexico, 17–22 October2010, IAHS Publ. 339, IAHS, Wallingford, UK, pp 27–32
Herrera G, Tomás R, Monells D, Centolanza G, Mallorquí JJ, Vicente F, Navarro VD, Lopez-Sanchez JM, Sanabria M, Cano M, Mulas J (2010) Analysis of subsidence using TerraSAR-X data: Murcia case study. Eng Geol 116(3–4):284–295. doi:10.1016/j.enggeo.2010.09.010
Heywood CE (1993) Monitoring aquifer compaction and land subsidence due to ground-water withdrawal in the El Paso, Texas - Juarez, Chihuahua area. In: Prince KR, Galloway DL, Leake SA (eds) US Geological Survey Subsidence Interest Group Conference, Edwards Air Force Base, Antelope Valley, Calif. 18–19 November 1992, abstracts and summary, US Geol Surv Open-File Rep 94–532, http://pubs.usgs.gov/of/1994/ofr94-532/. Cited 13 July 2011
Hoffmann J (2005) The future of satellite remote sensing in hydrogeology. Hydrogeol J 13(1):247–250. doi:10.1007/s10040-004-0409-2
Hoffmann J, Zebker HA (2003) Prospecting for horizontal surface displacements in Antelope Valley, California, using satellite radar interferometry. J Geophys Res 108(F1):6011. doi:10.1029/2003JF000055
Hoffmann J, Zebker HA, Galloway DL, Amelung F (2001) Seasonal subsidence and rebound in Las Vegas Valley, Nevada, observed by synthetic aperture radar interferometry. Water Resour Res 37(6):1551–1566
Hoffmann J, Galloway DL, Zebker HA (2003a) Inverse modeling of interbed storage parameters using land subsidence observations, Antelope Valley, California. Water Resour Res 39(2):SBH 5–1–5–10. doi:10.1029/2001WR001252
Hoffmann J, Leake SA, Galloway DL, Wilson AM (2003b) MODFLOW-2000 ground-water model—User guide to the subsidence and aquifer-system compaction (SUB) package. US Geol Surv Open-File Rep 03–233 version 1.1.1. http://pubs.usgs.gov/of/2003/ofr03-233/. Cited 13 July 2011
Hofton MA, Blair JB (2002) Laser altimeter return pulse correlation: a method for detecting surface topographic change. J Geodyn 34(3–4):477–489
Holzer TL (1981) Preconsolidation stress of aquifer systems in areas of induced land subsidence. Water Resour Res 17:693–704
Holzer TL (ed) (1984a) Man induced land subsidence. Geol. Soc of America, Washington, DC, 232 pp
Holzer TL (1998) History of the aquitard-drainage model in land subsidence case studies and current research. In: Borchers JW (ed) Land subsidence case studies and current research. Proceedings of the Dr. Joseph F. Poland Symposium on Land

Subsidence, vol 8. Sacramento, CA, 4–5 Oct 1995, Star, Belmont, CA, pp 7–12
Holzner J, Bamler R (2002) Burst-mode and scanSAR interferometry. IEEE Trans Geosci Rem Sens 40:1917–1934
Hooper A, Zebker HA, Segall P, Kampes B (2004) A new method for measuring deformation on volcanoes and other natural terrains using InSAR persistent scatterers. Geophys Res Lett 31: L23611. doi:10.1029/2004GL021737
Hooper A, Segall P, Zebker HA (2007) Persistent scatterer interferometric synthetic aperture radar for crustal deformation analysis, with application to Volcán Alcedo, Galápagos. J Geophys Res 112(B7):B07407. doi:10.1029/2006JB004763
Hsieh PA (1996) Deformation-induced changes in hydraulic head during ground-water withdrawal. Ground Water 36(6):1082–1089
Hung WC, Hwang C, Chang CP, Yen JY, Liu CH, Yang WH (2010) Monitoring severe aquifer-system compaction and land subsidence in Taiwan using multiple sensors: Yunlin, the southern Choushui River alluvial fan. Environ Earth Sci 59(7):1535–1548. doi:10.1007/s12665-009-0139-9
Hwang C, Hung WC, Liu CH (2008) Results of geodetic and geotechnical monitoring of subsidence for Taiwan High Speed Rail operation. Nat Hazards 47:1–16. doi:10.1007/s11069-007-9211-5
IAHS (1977) Proceedings of the Second International Symposium on Land Subsidence, Anaheim, Calif, Dec 1976. IAHS Publ. 121, IAHS, Wallingford, UK. http://iahs.info/redbooks/121.htm. Cited 13 July 2011
Ikehara ME, Phillips SP (1994) Determination of land subsidence related to ground-water level declines using global positioning system and leveling surveys in Antelope Valley, Los Angeles and Kern Counties, California, 1992. US Geol Surv Water Resour Invest Rep 94–4184. http://pubs.er.usgs.gov/usgspubs/wri/wri944184. Cited 13 July 2011
Ingebritsen SE, Sanford WE, Neuzil CE (2006) Groundwater in geologic processes, 2nd edn. Cambridge Univ. Press, New York
Jackson JD (2005) The role of poroviscosity in evaluating land subsidence due to groundwater extraction from sedimentary basin sequences. RMIT, Melbourne, Australia
Jackson JD, Helm DC, Brumley JC (2004) The role of poroviscosity in evaluating land subsidence due to groundwater extraction from sedimentary basin sequences. Geofís Int 43 (4):689–695
Jacob CE (1940) On the flow of water in an elastic artesian aquifer. Am Geophys Un:574–586
Jacob CE (1950) Flow of ground water. In: Rouse H (ed), Engineering hydraulics: Proceedings of the Fourth Hydraulics Conference, Iowa Institute of Hydraulic Research, Iowa City, IW, 12–15 June 1949
Jeng DI (2005) A three-dimensional model of poroviscous aquifer deformation. Virginia Tech, Blacksburg, VA
Johnson AI (ed) (1991) Land subsidence. Proceedings of the Fourth International Symposium on Land Subsidence, 12–17 May 1991, Houston, TX. IAHS Publ. 200. http://iahs.info/redbooks/200.htm. Cited 13 July 2011
Johnson AI, Carbognin L, Ubertini L (eds) (1986) Land subsidence. Proceedings of the Third International Symposium on Land Subsidence, Venice, Italy, Mar 1984. IAHS Publ. 151. http://iahs.info/redbooks/151.htm. Cited 13 July 2011
Jorgensen DG (1980) Relationships between basic soils-engineering equations and basic ground-water flow equations: US Geol Surv Water Suppl Pa 2064. http://pubs.er.usgs.gov/publication/wsp2064. Cited 13 July 2011
Kampes D (2005) Displacement parameter estimation using permanent scatterer interferometry: DLR-Forschungsberichte 16
Kasmarek MC, Strom EW (2002) Hydrogeology and simulation of ground-water flow and land-surface subsidence in the Chicot and Evangeline aquifers, Houston-Galveston region, Texas. US Geol Surv Water Resour Invest Rep 02–4022. http://pubs.usgs.gov/wri/wri024022/. Cited 13 July 2011
Kihm JH, Kim JM, Song SH, Lee GS (2007) Three-dimensional numerical simulation of fully coupled groundwater flow and land deformation due to groundwater pumping in an unsaturated fluvial aquifer system. J Hydrol 335:1–14
Kim JM (2005) Three-dimensional numerical simulation of fully coupled groundwater flow and land deformation in unsaturated true anisotropic aquifers due to groundwater pumping. Water Resour Res 41:W01003
Kim JM, Parizek RR (1999) A mathematical model for the hydraulic properties of deforming porous media. Ground Water 37(4):546–554
King NE, Argus D, Langbein J, Agnew DC, Bawden GW, Dollar RS, Liu Z, Galloway D, Reichard E, Yong A, Webb FH, Bock Y, Stark K, Barseghian D (2007) Space geodetic observation of expansion of the San Gabriel Valley, California, aquifer system, during heavy rainfall in winter 2004–2005. J Geophys Res 112: B03409. doi:10.1029/2006JB004448
Kircher M (2004) Analyse flächenhafter senkungserscheinungen in sedimentären gebieten mit den neuen techniken der radarfernerkundung am beispiel der Niederrheinischen bucht [Analysis of extensive subsidence in sedimentary areas with the new techniques of radar remote sensing using the example of the lower Rhine basin]. PhD Thesis, Universität Bonn, Germany
Konikow LF, Neuzil CE (2007) A method to estimate groundwater depletion from confining layers. Water Resour Res 43:W07417. doi:10.1029/2006WR005597
Kunisue S, Kokubo T (2010) In situ formation compaction monitoring in deep reservoirs using optical fibres. In: Carreón-Freyre D, Cerca M, Galloway DL, Silva-Corona JJ (eds), Land subsidence, associated hazards and the role of natural resources development (EISOLS 2010). IAHS Publ. 339, IAHS, Wallingford, UK, pp 368–370
Larson KJ, Basagaolu H, Mario M (2001) Numerical simulation of land subsidence in the Los Banos-Kettleman City area, California. University of California Davis Water Resources Center technical completion report contribution 207. http://escholarship.org/uc/item/5h60p535?query=larson%20keith. Cited 13 July 2011
Leake SA (1990) Interbed storage changes and compaction in models of regional ground-water flow. Water Resour Res 26 (9):1939–1950
Leake SA (1991) Simulation of vertical compaction in models of regional ground-water flow. In: Johnson AI (ed) Land subsidence. Proceedings of the Fourth International Symposium on Land Subsidence, 12–17 May 1991, Houston, TX. IAHS Publ. 200, pp 565–574. http://iahs.info/redbooks/a200/iahs_200_0565.pdf. Cited 13 July 2011
Leake SA, Galloway DL (2007) MODFLOW ground-water mode: user guide to the Subsidence and Aquifer-System Compaction Package (SUB-WT) for water-table aquifers. USGS Tech and Methods Rep 6–A23. http://pubs.usgs.gov/tm/2007/06A23/. Cited 13 July 2011
Leake SA, Galloway DL (2010) Use of the SUB-WT Package for MODFLOW to simulate aquifer-system compaction in Antelope Valley, California, USA. In: Carreón-Freyre D, Cerca M, Galloway DL (eds) Land subsidence, associated hazards and the role of natural resources development: proceedings. Eighth International Symposium on Land Subsidence, Santiago de Querétaro, Mexico, 17–22 October 2010, IAHS Publ. 339, pp 61–67
Leake SA, Prudic DE (1991) Documentation of a computer program to simulate aquifer-system compaction using the modular finite-difference ground-water flow model. US Geol Surv Tech Water Resour Invest, book 6, chap. A2. http://pubs.usgs.gov/twri/twri6a2/. Cited 13 July 2011
Leighton DA, Phillips SP (2003) Simulation of ground-water flow and land subsidence in the Antelope Valley ground-water basin, California. US Geol Surv Water Resour Invest Rep 03–4016. http://pubs.usgs.gov/wri/wrir034016/text.html. Cited 13 July 2011
Leva D, Nico G, Tarchi D, Fortuny-Guasch J, Sieber AJ (2003) Temporal analysis of a landslide by means of a ground-based SAR Interferometer. IEEE Trans Geosci Remote Sens 41 (4):745–752

Li J (2000) A nonlinear elastic solution for subsidence due to ASR applications to multi-aquifer systems. In: Carbognin L, Gambolati G, Johnson AI (eds) Land subsidence. Proceedings of the Sixth International Symposium on Land Subsidence, vol 2, Ravenna, Italy, 24–29 Sept 2000, La Garagolav, Padova, Italy, pp 331–342

Li J (2003) A nonlinear elastic solution of 1-D subsidence due to aquifer storage and recovery applications. Hydrogeol J 11:646–658

Li J (2007a) Transient radial movement of a confined leaky aquifer due to variable well flow rates. J Hydrol 333(2–4):542–553

Li J (2007b) Analysis of radial movement of an unconfined leaky aquifer due to pumping and injection. Hydrogeol J 15(6):1063–1076

Li J (2007c) Analysis of radial movement of a confined aquifer due to pumping and injection. Hydrogeol J 15(3):442–458

Li J, Helm DC (1995) A general formulation for aquifer deformation under dynamic and viscous conditions. In: Barends FBJ, Brouwer FJJ, Schröder FH (eds) Land subsidence. Proceedings of the Fifth International Symposium on Land Subsidence, The Hague, Netherlands, October 1995. IAHS Publ. 234, pp 323–332. http://iahs.info/redbooks/a234/iahs_234_0323.pdf. Cited 13 July 2011

Li J, Helm DC (1997) Numerical formulation of dynamic behavior within saturated soil characterized by elasto-viscous behavior with an application to Las Vegas Valley. In: Yuan J (ed) Computer method and advances in geomechanics. Proceedings of the 9th International Conference of the International Association for Computer Method and Advances in Geomechanics, vol 2, Wuhan, China, Balkema, Rotterdam, pp 911–916

Li J, Helm DC (1998) A theory for dynamic motion of saturated soil characterized by viscous behavior. In: Borchers J (ed) Land subsidence case histories and current research. Proceedings of the Dr. Joseph F. Poland Symposium on Land Subsidence. Spec. Publ. 8, Assoc. Eng. Geol., Denver, CO, pp 356–407

Li J, Helm DC (2000) Nonlinear viscous model for aquifer compression associated with ASR applications. In: Carbognin L, Gambolati G, Johnson AI (eds) Land subsidence. Proceedings of the Sixth International Symposium on Land Subsidence, vol 2, Ravenna, Italy, 24–29 Sept 2000, La Garagolav, Padova, Italy, pp 319–330

Li J, Helm DC (2001a) Using an analytical solution to estimate the subsidence risk caused by ASR applications. J Env Eng Geosci 7(1):67–79

Li J, Helm DC (2001b) Elastic solutions of 1-D subsidence due to ASR applications. Proceedings of the World Water and Environmental Resources Congress. Paper No. 206, EWRI-ASCE, Orlando, FL

Li J, Helm DC (2001c) A nonlinear elasto-viscous model for subsidence due to artificial recharge-discharge. Proceedings of the 36th Symposium on Geological Engineering and Geotechnical Engineering, University of Nevada Las Vegas, Las Vegas, NV, pp 437–446

Liu Y, Helm DC (2008a) Inverse procedure for calibrating parameters that control land subsidence caused by subsurface fluid withdrawal: 1. Methods. Water Resour Res 44:W07423. doi:10.1029/2007WR006605

Liu Y, Helm DC (2008b) Inverse procedure for calibrating parameters that control land subsidence caused by subsurface fluid withdrawal: 2. field application. Water Resour Res 44: W07424. doi:10.1029/2007WR006606

Liu CH, Pan YW, Liao JJ, Hung WC (2004) Estimating coefficients of volume compressibility from compression of strata and piezometric changes in multiaquifer system in west Taiwan. Eng Geol 75:33–47. doi:10.1016/j.enggeo.2004.04.007

Lofgren BE (1969) Field measurement of aquifer-system compaction, San Joaquin Valley, California, U.S.A. In: Tison LJ (ed) Land subsidence. Proceedings of the Tokyo Symposium, Sept 1969, IAHS Publ. 88, pp 272–284. http://iahs.info/redbooks/a088/088031.pdf. Cited 13 July 2011

Lu Z, Dzurisin D, Jung HS, Zhang JX, Zhang YH (2010) Radar image and data fusion for natural hazards characterization. Int J Image Data Fusion 1:217–242

Lubis AM, Sato T, Tomiyama N, Isezaki N, Yamanokuchi T (2011) Ground subsidence in Semarang-Indonesia investigated by ALOS–PALSAR satellite SAR interferometry. J Asian Earth Sci 40:1079–1088. doi:10.1016/j.jseaes.2010.12.001

Massonnet D, Feigl KL (1998) Radar interferometry and its application to changes in the earth's surface. Rev Geophys 36:441–500

McDonald MG, Harbaugh AW (1988) A modular three-dimensional finite-difference ground-water flow model. US Geol Surv Tech Water Resour Inv, book 6, chap. A1 [also available in Chinese]. http://pubs.usgs.gov/twri/twri6a1/. Cited 13 July 2011

Meinzer OE (1928) Compressibility and elasticity of artesian aquifers. J Geol 23(3):263–291

Meinzer OE, Hard HA (1925) The artesian-water supply of the Dakota Sandstone in North Dakota with special reference to the Edgeley Quadrangle. US Geol Surv Water Suppl Pap 520-E:73–96

Metzger LF, Ikehara ME, Howle JF (2002) Vertical-deformation, water-level, microgravity, geodetic, water-chemistry, and flow-rate data collected during injection, storage, and recovery tests at Lancaster, Antelope Valley, California, September 1995 through September 1998. US Geol Surv Open-File Rep 01–414. http://pubs.usgs.gov/of/2001/ofr01414/. Cited 13 July 2011

Meyer WR, Carr JE (1979) A digital model for simulation of ground-water hydrology in the Houston area, Texas. US US Geol Surv Open-File Rep 79–677

Miura N, Hayashi S, Madhav MR, Hachiya Y (1995) Problems of subsidence and their mitigation in Saga Plain, Japan. In: Barends FBJ, Brouwer FJJ, Schröder FH (eds) Land subsidence. Proceedings of the Fifth International Symposium on Land Subsidence, vol 2. October 1995, The Hague, Netherlands. IAHS Publ. 234, pp 463–469. http://iahs.info/redbooks/a234/iahs_234_0463.pdf. Cited 13 July 2011

Morgan DS, Dettinger MD (1996) Ground-water conditions in Las Vegas Valley, Clark County, Nevada, part 2: hydrogeology and simulation of ground-water flow. US Geol Surv Water Suppl Pap 2320-B. http://pubs.er.usgs.gov/usgspubs/wsp/wsp2320B. Cited 13 July 2011

Motagh M, Djamour Y, Walter TR, Wetzel H-U, Zschau J, Arabi S (2007) Land subsidence in Mashhad Valley, northeast Iran: results from InSAR, levelling and GPS. Geophys J Int 168:518–526. doi:10.1111/j.1365-246X.2006.03246.x

Narasimhan TN, Witherspoon PA (1977) Numerical model for land subsidence in shallow groundwater systems. Proceedings of the Second International Symposium on Land Subsidence, Anaheim, CA, December 1976, IAHS Publ. 121, pp 133–144. http://iahs.info/redbooks/a121/iahs_121_0133.pdf. Cited 13 July 2011

National Research Council (1991) Mitigating losses from land subsidence in the United States. National Academy Press, Washington, DC

Neuman SP, Witherspoon PA (1972) Field determination of hydraulic properties of leaky multiple aquifer systems. Water Resour Res 8(5):1284–1298

Neuman SP, Preller C, Narasimhan TN (1982) Adaptive explicit-implicit quasi three-dimensional finite element model of flow and subsidence in multiaquifer systems. Water Resour Res 18 (5):1551–1561

Neuzil CE (1986) Groundwater flow in low-permeability environments. Water Resour Res 22(8):1163–1195

Nishikawa T, Rewis DL, Martin P (2001) Numerical simulation of ground-water flow and land subsidence at Edwards Air Force Base, Antelope Valley, California. US Geol Surv Water Resour Invest Rep 01–4038

NOAA (2011) CORS: Continuously Operation Reference Station. National Geodetic Survey, National Oceanic and Atmospheric Administration, Washington, DC. http://www.ngs.noaa.gov/CORS/. Cited 13 July 2011.

Ortega-Guerrero A, Rudolph DL, Cherry JA (1999) Analysis of long-term land subsidence near Mexico City: field investigations and predictive modeling. Water Resour Res 35(11):3327–3341

Osmanoglu B, Dixon TH, Wdowinski S, Cabral-Cano E, Jiang Y (2011) Mexico City subsidence observed with persistent scatterer InSAR. Int J Appl Earth Obs 13:1–12. doi:10.1016/j.jag.2010.05.009

Pavelko MT (2000) Ground-water and aquifer-system-compaction data from the Lorenzi Site, Las Vegas, Nevada, 1994–99. US Geol Surv Open-File Rep 00–362. http://pubs.er.usgs.gov/usgspubs/ofr/ofr00362. Cited 13 July 2011

Pavelko MT (2003) Estimates of hydraulic properties from a one-dimensional numerical model of vertical aquifer-system deformation, Lorenzi Site, Las Vegas, Nevada. US Geol Surv Water Resour Invest Rep 03–4083. http://pubs.usgs.gov/wri/wri034083/index.html. Cited 13 July 2011

Pavelko, MT, Hoffmann, J, Damar, NA (2006) Interferograms showing land subsidence and uplift in Las Vegas Valley, Nevada, 1992–99. US Geol Surv Sci Invest Rep 2006–5218. http://pubs.usgs.gov/sir/2006/5218/. Cited 13 July 2011

Phien-wej N, Giao PH, Nutalaya P (2006) Land subsidence in Bangkok, Thailand. Eng Geol 82:187–201

Phillips SP, Carlson CS, Metzger LF, Howle JF, Galloway DL, Sneed M, Ikehara ME, Hudnut KW, King NE (2003) Analysis of tests of subsurface injection, storage, and recovery of freshwater in Lancaster, Antelope Valley, California. US Geol Surv Water Resour Invest Rep 03–4061. http://ca.water.usgs.gov/pubs/wrir_03-4061.html. Cited 13 July 2011

Poland JF (ed) (1984) Guidebook to studies of land subsidence due to ground-water withdrawal. UNESCO Studies and Reports in Hydrology 40, UNESCO, Paris. http://wwwrcamnl.wr.usgs.gov/rgws/Unesco/. Cited 13 July 2011

Poland JF, Davis GH (1969) Land subsidence due to withdrawal of fluids. Rev Eng Geol 2:187–269

Pope JP, Burbey TJ (2003) Characterization and modeling of land subsidence due to ground-water withdrawals from the confined aquifers of the Virginia Coastal Plain. In: Prince KR, Galloway DL (eds) U.S. Geological Survey Subsidence Interest Group Conference, Proceedings of the technical meeting, Galveston, Texas, 27–29 Nov 2001. US Geol Surv Open-File Rep 03–308:49–56. http://pubs.usgs.gov/of/2003/ofr03-308/. Cited 13 July 2011

Pope JP, Burbey TJ (2004) Multiple-aquifer characterization from single borehole extensometer records. Ground Water 42(1):45–58

Prince KR, Galloway DL (eds) (2003) U.S. Geological Survey Subsidence Interest Group Conference, Proceedings of the Technical Meeting, 27–29 Nov 2001, Galveston, TX. US Geol Surv Open-File Rep 03–308. http://pubs.usgs.gov/of/2003/ofr03-308/. Cited 13 July 2011

Prince KR, Leake SA (eds) (1997) U.S. Geological Survey Subsidence Interest Group Conference, Proceedings of the technical meeting, Las Vegas, NV, 14–16 Feb 1995. US Geol Surv Open-File Rep 97–47. http://pubs.usgs.gov/of/1997/ofr97-047/. Cited 13 July 2011

Prince KR, Galloway DL, Leake SA (eds) (1995) U.S. Geological Survey Subsidence Interest Group Conference, Edwards Air Force Base, Antelope Valley, California, 18–19 Nov 1992: abstracts and summary. US Geol Surv Open-File Rep 94–532. http://pubs.usgs.gov/of/1994/ofr94-532/. Cited 13 July 2011

Reeves J, Knight RJ, Zebker HA, Schreüder W, Agram PS, Lauknes T (2010) InSAR data produce specific storage estimates for an agricultural area in the San Luis Valley, Colorado. AGU Fall Meeting 2010, abstract no. H11K-08, AGU, Washington, DC

Riley FS (1969) Analysis of borehole extensometer data from central California. In: Tison LJ (ed) Land subsidence. Proceedings of the Tokyo Symposium, Sept 1969, IAHS Pub. 88:423–431. http://iahs.info/redbooks/a088/088047.pdf. Cited 13 July 2011

Riley FS (1986) Developments in borehole extensometry. In: Johnson AI, Carbognin L, Ubertini L (eds) Land subsidence. Proceedings of the Third International Symposium on Land Subsidence, Venice, Italy, March 1984, IAHS Pub. 151, pp 169–186. http://iahs.info/redbooks/a151/iahs_151_0169.pdf. Cited 13 July 2011

Riley FS (1998) Mechanics of aquifer systems: the scientific legacy of Joseph F. Poland. In: Borchers JW (ed) Land subsidence case studies and current research. Proceedings of the Dr. Joseph F. Poland Symposium on Land Subsidence, vol 8, 4–5 Oct 1995, Sacramento, CA, Star , Belmont, CA, pp 13–27

Sæbø TO (2010) Seafloor depth estimation by means of interferometric synthetic aperture sonar. PhD Thesis, University of Tromsø, Norway. http://munin.uit.no/munin/bitstream/10037/2793/3/thesis.pdf. Cited 13 July 2011

Sandhu RS (1979) Modeling land subsidence. In: Saxena SK (ed) Evaluation and prediction of subsidence. American Soc. of Civil Eng., Washington, DC

Schmidt DA, Bürgmann R (2003) Time dependent land uplift and subsidence in the Santa Clara Valley, California, from a large InSAR data set. J Geophys Res 108(B9). doi:10.1029/2002JB002267

Schomaker MC, Berry RM (1981) Geodetic leveling. NOAA Manual NOS NGS 3. http://www.ngs.noaa.gov/PUBS_LIB/Geodeticleveling_nos_3.pdf. Cited 13 July 2011

Scott RF (1963) Principles of soil mechanics. Addison, Palo Alto, CA

Shearer TR (1998) A numerical model to calculate land subsidence, applied at Hangu in China. Eng Geol 49:85–93

Sheng Z, Helm DC, Li J (2003) Mechanisms of earth fissuring caused by groundwater withdrawal. Env Eng Geosci 9(4):313–324

Singh B, Saxena NC (1991) Land Subsidence. International Symposium, 11–15 Dec, 1989. Central Mining Research Station (Dhanbad, India). Balkema, Rotterdam, the Netherlands

Sneed M (2010) Measurement of land subsidence using interferometry, Coachella Valley, California. In: Carreón-Freyre D, Cerca M, Galloway DL, Silva-Corona JJ (eds) Land subsidence, associated hazards and the role of natural resources development (EISOLS 2010). IAHS Publ. 339, pp 260–263

Sneed M, Brandt JT (2007) Detection and measurement of land subsidence using global positioning system surveying and interferometric synthetic aperture radar, Coachella Valley, California, 1996–2005. US Geol Surv Sci Invest Rep 2007–5251. http://pubs.usgs.gov/sir/2007/5251/. Cited 13 July 2011

Sneed M, Galloway DL (2000) Aquifer-system compaction and land subsidence: measurements, analyses, and simulations: the Holly site, Edwards Air Force Base, Antelope Valley, California. US Geol Surv Water-Resour Invest Rep 00–4015. http://pubs.usgs.gov/wri/2000/wri004015/. Cited 13 July 2011

Taylor DW (1948) Fundamentals of soil mechanics. Wiley, New York, p 700

Teatini P, Tosi L, Strozzi T, Carbognin L, Wegmüller U, Rizzetto F (2005) Mapping regional land displacements in the Venice coastland by an integrated monitoring system. Rem Sens Env 98. doi:10.1016/j.rse.2005.08.002

Terzaghi K (1923) Die berechnung der durchlässigkeitziffer des tones aus dem verlauf der hydrodymanischen spannungserscheinungen [The computation of permeability of clays from the progress of hydrodynamic strain]. Sitzungsberichte, Mathematisch-naturwissenschaftliche Klasse, Part IIa 132, Akademie der Wissenschaften, Vienna, pp 125–138

Terzaghi K (1925) Settlement and consolidation of clay. McGraw-Hill, New York, pp 874–878

Therrien R, McLaren RG, Sudicky EA, Panday SM (2010) HydroGeoSphere: a three-dimensional numerical model describing fully-integrated subsurface and surface flow and solute transport (draft edition 23 July 2010). Groundwater Simulations Group, University of Waterloo, Waterloo, ON. http://hydrogeosphere.org/. Cited 13 July 2011

Tison LJ (ed) (1969) Land subsidence. Proceedings of the Tokyo Symposium, Sept 1969, UNESCO Studies and Reports in Hydrology 8, IAHS Pub., pp 88–89. http://iahs.info/redbooks/088.htm. Cited 13 July 2011

Tolman CF, Poland JF (1940) Ground-water, salt-water infiltration, and ground-surface recession in Santa Clara Valley, Santa Clara County, California. Trans Am Geophys Union 1:23–35

Usai S (2001) A new approach for long term monitoring of deformations by differential SAR interferometry. PhD Thesis, Technische Universiteit Delft, the Nederlands

Verruijt A (1969) Elastic storage of aquifers. In: De Wiest RJM (ed) Flow through porous media. Academic, New York

Wang HF (2000) Theory of linear poroelasticity with applications to geomechanics and hydrogeology. Princeton University Press, Princeton, NJ

Wang GY, You G, Shi B, Yu J, Tuck M (2009) Long-term land subsidence and strata compression in Changzhou, China. Eng Geol 104:109–118

Werner C, Wegmüller U, Strozzi T, Wiesmann A (2003) Interferometric point target analysis for deformation mapping. Proc 2003 IEEE Int. Geoscience Remote Sensing Symp., vol 7, pp 4362–4364. doi:10.1109/IGARSS.2003.1295516

Werner C, Strozzi T, Wiesmann A, Wegmuller U (2008) A real-aperture radar for ground-based differential interferometry. Proc 2008 IEEE Int Geosci Remote Sensing Symposium, vol 3, Boston, MA, July 2008, pp 210–213. doi:10.1109/IGARSS.2008.4779320

Wildermuth Environmental Inc (2006) Chino Basin optimum basin management program: management zone 1 interim monitoring program—MZ1 summary report, prepared for the MZ-1 Technical Committee, Wildermuth, Lake Forest, CA

Williamson AK, Prudic DE, Swain LA (1989) Ground-water flow in the Central Valley, California: US Geol Surv Prof Pap 1401-D. http://pubs.er.usgs.gov/usgspubs/pp/pp1401D. Cited 13 July 2011

Wilson AM, Gorelick S (1996) The effects of pulsed pumping on land subsidence in the Santa Clara Valley, California. J Hydrol 174:375–396

Wisely BA, Schmidt D (2010) Deciphering vertical deformation and poroelastic parameters in a tectonically active fault-bound aquifer using InSAR and well level data, San Bernardino basin, California. Geophys J Int 181(3):1185–1200

Witherspoon PA, Freeze RA (1972) The role of aquitards in a multiple-aquifer system. Geotimes 17(4):22–24

Wolff RG (1970) Relationship between horizontal strain near a well and reverse water-level fluctuations. Water Resour Res 6:1721–1728

Worawattanamateekul J, Hoffmann J, Adam N et al (2004) Radar interferometry technique for urban subsidence monitoring: a case study in Bangkok and its vicinity. ENVISAT Symposium 2004, Salzburg, Austria, 6–10 Sept 2004

Zhang A, Gong S, Carbognin L, Johnson AI (eds) (2005) Land subsidence. Proceedings of the 7th International Symposium on Land Subsidence, Oct 2005, vols 1–2. Shanghai Scientifi, Shanghai, PRC

Zhao C-Y, Zhang Q, Yang C, Zou W (2011) Integration of MODIS data and Short Baseline Subset (SBAS) technique for land subsidence monitoring in Datong, China. J Geodyn 52:16–23. doi:10.1016/j.jog.2010.11.004

Zilkoski DB, D'Onofrio JD, Frakes SJ (1997) Guidelines for establishing GPS-derived ellipsoid heights (standards: 2cm and 5cm), ver. 4.3. NOAA Technical Memorandum NOS NGS-58. http://geodesy.noaa.gov/PUBS_LIB/NGS-58.pdf. Cited 13 July 2011

Zilkoski DB, Hall LW, Mitchell GJ et al (2003) The Harris-Galveston Coastal Subsidence District/National Geodetic Survey automated GPS subsidence monitoring project. In: Prince KR, Galloway DG (eds) U.S. Geological Survey Subsidence Interest Group Conference, Proceedings of the technical meeting, Galveston, TX, 27–29 Nov 2001. US Geol Surv Open-File Rep 03–308. http://pubs.usgs.gov/of/2003/ofr03-308/. Cited 13 July 2011

Zilkoski DB, Carlson EE, Smith CL (2008) Guidelines for establishing GPS-derived orthometric heights (standards: 2 cm and 5 cm), ver. 4.3. NOAA Technical Memorandum NOS NGS-59. http://www.ngs.noaa.gov/PUBS_LIB/NGS592008069FINAL2.pdf. Cited 30 July 2011 . Cited 13 July 2011